Molecular Vision 2016; 22:472-490 <http://www.molvis.org/molvis/v22/472>
Received 25 January 2016 | Accepted 13 May 2016 | Published 16 May 2016

Gene expression changes in the retina following subretinal injection of human neural progenitor cells into a rodent model for retinal degeneration

Melissa K. Jones,[1,2] Bin Lu,[1,2] Mehrnoosh Saghizadeh,[1,2,3] Shaomei Wang[1,2,3]

[1]Department of Biomedical Sciences, Cedars-Sinai Medical Center, Los Angeles, CA; [2]Eye Program, Board of Governors Regenerative Medicine Institute, Cedars-Sinai Medical Center, Los Angeles, CA; [3]David Geffen School of Medicine, University of California Los Angeles, Los Angeles, CA

Purpose: Retinal degenerative diseases (RDDs) affect millions of people and are the leading cause of vision loss. Although treatment options for RDDs are limited, stem and progenitor cell–based therapies have great potential to halt or slow the progression of vision loss. Our previous studies have shown that a single subretinal injection of human forebrain derived neural progenitor cells (hNPCs) into the Royal College of Surgeons (RCS) retinal degenerate rat offers long-term preservation of photoreceptors and visual function. Furthermore, neural progenitor cells are currently in clinical trials for treating age-related macular degeneration; however, the molecular mechanisms of stem cell–based therapies are largely unknown. This is the first study to analyze gene expression changes in the retina of RCS rats following subretinal injection of hNPCs using high-throughput sequencing.

Methods: RNA-seq data of retinas from RCS rats injected with hNPCs (RCS^{hNPCs}) were compared to sham surgery in RCS (RCS^{sham}) and wild-type Long Evans (LE^{sham}) rats. Differential gene expression patterns were determined with in silico analysis and confirmed with qRT-PCR. Function, biologic, cellular component, and pathway analyses were performed on differentially expressed genes and investigated with immunofluorescent staining experiments.

Results: Analysis of the gene expression data sets identified 1,215 genes that were differentially expressed between RCS^{sham} and LE^{sham} samples. Additionally, 283 genes were differentially expressed between the RCS^{hNPCs} and RCS^{sham} samples. Comparison of these two gene sets identified 68 genes with inverse expression (termed rescue genes), including *Pdc*, *Rp1*, and *Cdc42ep5*. Functional, biologic, and cellular component analyses indicate that the immune response is enhanced in RCS^{sham}. Pathway analysis of the differential expression gene sets identified three affected pathways in RCS^{hNPCs}, which all play roles in phagocytosis signaling. Immunofluorescent staining detected the increased presence of macrophages and microglia in RCS^{sham} retinas, which decreased in RCS^{hNPCs} retinas similar to the patterns detected in LE^{sham}.

Conclusions: The results from this study provide evidence of the gene expression changes that occur following treatment with hNPCs in the degenerating retina. This information can be used in future studies to potentially enhance or predict responses to hNPC and other stem cell therapies for retinal degenerative diseases.

Retinal degenerative diseases (RDDs), such as retinitis pigmentosa (RP) and age-related macular degeneration (AMD), are characterized by progressive loss of photoreceptors and are the leading causes of vision loss in developed countries [1]. The pathophysiology of RDDs varies, encompassing hereditary contributions and environmental risk factors, thus complicating the diagnostic and treatment regimen. RP is an inherited disorder with known mutations in more than 70 genes that cause abnormalities in photoreceptors or RPE cells, leading to progressive vision loss [2]. Conversely, several dietary- and lifestyle-related risk factors [3,4] and a few known genetic components [5-8] lead to vision loss in AMD. Currently, there are no effective treatments for most RDDs, and no therapies are able to reverse the degeneration of vision.

Stem cell–based therapies offer the potential to treat several diseases, including RDDs. The benefits of stem cell–based approaches include therapeutic longevity, a range of cell sources (e.g., embryonic, fetal, adult, and induced pluripotent stem cells), and the only available option for some patients with RDDs. Two main therapeutic strategies have evolved with the use of stem cells. In replacement therapies, stem cell–derived retinal cells act to replace the degenerating retina, although the longevity, cell orientation, intervention timing, and integration of these cells are still in question. The second strategy is to use non-retinal lineage stem cells in a neurosupportive role to halt or slow the progression of degeneration, thus preserving the remaining visual function. Although current clinical trials using neural stem cells

Correspondence to: Shaomei Wang, Cedars-Sinai Medical Center, Board of Governors Regenerative Medicine Institute, 8700 Beverly Boulevard, Los Angeles, CA, 90048; Phone: (310) 248-8576; FAX: (310) 248-8555; email: shaomei.wang@cshs.org

are being tested for safety [9], another clinically relevant stem cell population under investigation is human neural progenitor cells (hNPCs). Previous studies have shown that hNPCs provide photoreceptor neuroprotection and preserve visual function in retinal degenerate animal models [10-12]. In addition to neuroprotective effects, hNPCs have long-term survival, cause no immune-related pathology [12,13], have little proliferate capacity [11], and survive in nonhuman primates without immunosuppression [13]. Decidedly, hNPCs have all the factors that are crucial for transplantation into humans.

Proposed mechanisms of supportive stem cell–based therapies include growth factor release, regulation of endogenous protein expression, and restoration of cell-to-cell interactions, yet the mode of action is largely unestablished. Photoreceptor survival directly correlates to areas with grafted hNPCs [14,15], which have been shown to phagocytose photoreceptor outer segment debris in vivo [15,16] and have a greater effect when expressing certain neurotrophic growth factors [14]. Although hNPCs are able to impart a paracrine signaling effect on the retina, another major contributor to the preservation of vision is the retinal host tissue response to the stem cells [17,18]. Evidence suggests that exogenous stem cells can have a distal effect on retinal survival by inducing neurotrophic factor production by the retina [19,20] and are able to trigger regeneration in endogenous cells [21]. There may also be an indirect effect on other retinal cells, such as Müller glia, that induce photoreceptor survival. The dynamics of the injected stem cells and host tissue must be collaborative and synergistic for the maintenance of the host tissue; however, to what extent this occurs is unknown.

Knowing the gene expression profiles of the retina and the changes that occur during retinal degeneration is vital in creating targeted and more efficacious therapies. Previous studies have detected gene expression changes in human AMD retinas [22,23] and animal models of retinal degeneration [24,25]. Another clinically relevant animal model is the Royal College of Surgeons (RCS) rat, which is commonly used in preclinical testing of RDD therapies. RCS

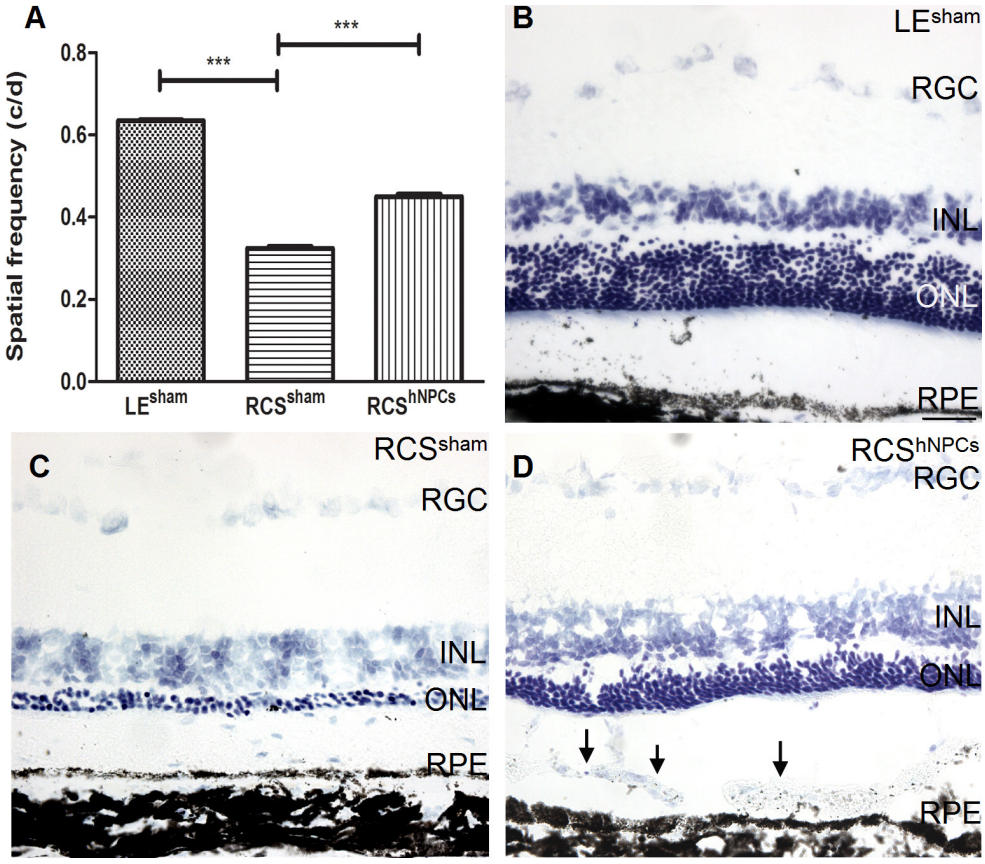

Figure 1. hNPCs aid in visual function preservation and photoreceptor survival in RCS rats. **A**: Optokinetic response (OKR) measurements showed that subretinal injection of human forebrain derived neural progenitor cells (hNPCs) into Royal College of Surgeons (RCS) rats (RCS^{hNPCs}) at P21 had a higher relative visual acuity (0.4503 ± 0.0064 c/d) compared to the RCS^{sham} rats (0.3245 ± 0.0047 c/d), though lower than LE^{sham} (0.6350 ± 0.0020 c/d); ***p<0.001. **B**: Histological analysis of the retinal sections of the LE^{sham} rats had approximately ten layers of photoreceptor cells in the outer nuclear layer (ONL). **C**: In contrast, the RCS^{sham} rats had three photoreceptor cell layers. **D**: Transplanted hNPCs (arrows) survived in the subretinal space of the RCS rats and preserve approximately five to six photoreceptor cell layers. RGC = retinal ganglion cell layer, INL = inner nuclear layer, ONL =outer nuclear layer. Scale bar = 25 µm.

rats have slow, progressive photoreceptor degeneration due to a mutation in the *Mertk* gene, which is expressed by RPE cells and is important in the binding of shed photoreceptor outer segments for proper phagocytosis [26,27]. The global transcriptome of the RCS rat has not been studied, and this knowledge could contribute to understanding the process of retinal degeneration. Furthermore, MERTK mutations have been detected in a subset of patients with retinitis pigmentosa [28], thus stressing the need for better understanding of this animal model as it relates to human disease.

A greater understanding of the molecular changes that occur during photoreceptor degeneration and how these changes are affected following stem-cell transplantation may enhance future stem cell treatments. This study aims to identify the gene expression changes that occur following treatment of hNPCs in the RCS rat, a rodent model for retinal degeneration. hNPCs provided a functional benefit in slowing vision loss, and histological analysis showed that hNPCs aided in photoreceptor survival. Transcriptome-wide profiling of gene expression by RNA-sequencing (RNA-seq) showed that there are differentially expressed genes in the retinas of wild-type Long Evans (LE^{sham}) versus RCS^{sham} rats and in RCS rats following injection of hNPCs (RCS^{hNPCs}). From this gene set, 68 genes were shown to have inverse relationships between LE^{sham} versus RCS^{sham} and RCS^{sham} versus RCS^{hNPCs} comparisons, suggesting that the expression of these genes is rescued with treatment of hNPCs. Bioinformatic analyses of functional, biologic, and cellular components indicate an increase in immune response in RCS^{sham}. Additionally, differentially expressed genes were found to correlate to three signaling pathways, and expression levels were validated with qRT-PCR analysis. The affected pathways indicate that there is a modulation of phagocytosis signaling due to the decrease in phagocytic cells in the retina following subretinal transplantation of hNPCs. Immunofluorescent staining experiments revealed increases in macrophages and microglia in RCS^{sham} and a subsequent decrease in RCS^{hNPCs}, suggesting that hNPCs aid in immunomodulation. The information from this study will aid in a better understanding of the pathogenesis of retinal degeneration and the changes that occur following treatment with hNPCs.

METHODS

Derivation, maintenance, and transplantation of hNPCs: Human neural progenitor cells (hNPCs) isolated from fetal cortical brain tissue were obtained with institutional review board approval and in accordance with the National Institutes of Health guidelines for the collection of such tissues. hNPCs were cultured as neurospheres in Stemline Neural Stem Cell Expansion Medium (Sigma-Aldrich, St. Louis, MO) supplemented with 20 ng/ml epidermal growth factor (Sigma-Aldrich) and 10 ng/ml leukemia inhibitor factor (Millipore, Billerica, MA) as previously described [12]. Neurospheres of hNPCs at passage 23–25 were dissociated into a single cell suspension by incubation at 37 °C for 10 min with Accutase (Sigma-Aldrich) followed by trypsin inhibitor (Sigma-Aldrich) for 5 min and DNase (Sigma-Aldrich) for 10 min with gentle trituration in PBS (1X; 120 mM NaCl, 20 mM KCl, 10 mM $NaPO_4$, 5 mM KPO_4, pH 7.4; Life Technologies, Paisley, UK). An injection of 4×10^4 cells/eye in 2 µl of balanced salt solution (BSS) cell carrying medium (Alcon, Fort Worth, TX) was delivered to the subretinal space through a glass micropipette, as previously described [12]. Rats receiving a sham surgery were injected with BSS cell carrying medium alone.

Animals: Retinal degenerate RCS rats (n = 8) received a subretinal injection of hNPCs into one eye (RCS^{hNPCs}) and either sham surgery (RCS^{sham}; n = 4) or no treatment (n = 4) in the fellow eye at postnatal day 21 (P21). Long Evans (LE) rats (n = 3) received subretinal sham surgery (LE^{sham}) of cell carrying media into one eye, and the fellow eye received no treatment at P21. All rats received dexamethasone intraperitoneal injections for 2 weeks (2.5 mg/kg/day) following subretinal injection and cyclosporine A (Novartis, Basel, Switzerland) in the drinking water (210 mg/l) until the rats were euthanized at P60 following the functional studies. This study adhered to the Association for Research in Vision and Ophthalmology Statement for the Use of Animals in Ophthalmic and Vision research and was conducted with the approval of the Institutional Animal Care and Use Committee at Cedars-Sinai Medical Center.

Visual function testing: The optokinetic response (OKR) testing apparatus comprises a rotating cylinder displaying a vertical sine wave grating presented in virtual three-dimensional space on four computer monitors arranged in a square. Unrestrained rats were placed on a platform in the center of the square and tracked the grating with reflexive head movements. Visual acuity was quantified by increasing the spatial frequency of the grating until an OKR could no longer be elicited. Statistical analyses were performed with one-way ANOVA (ANOVA) and Newman-Keuls multiple comparison test using GraphPad Prism 5.01 (GraphPad Software, La Jolla, CA). Data were expressed as mean ± standard error of the mean (SEM), and a p value of less than 0.05 was considered statistically significant.

Tissue extraction and preparation: Eyes were enucleated from rats at age P60–64. For histology staining, eyes were fixed with 4% paraformaldehyde (Sigma-Aldrich) for 1 h followed

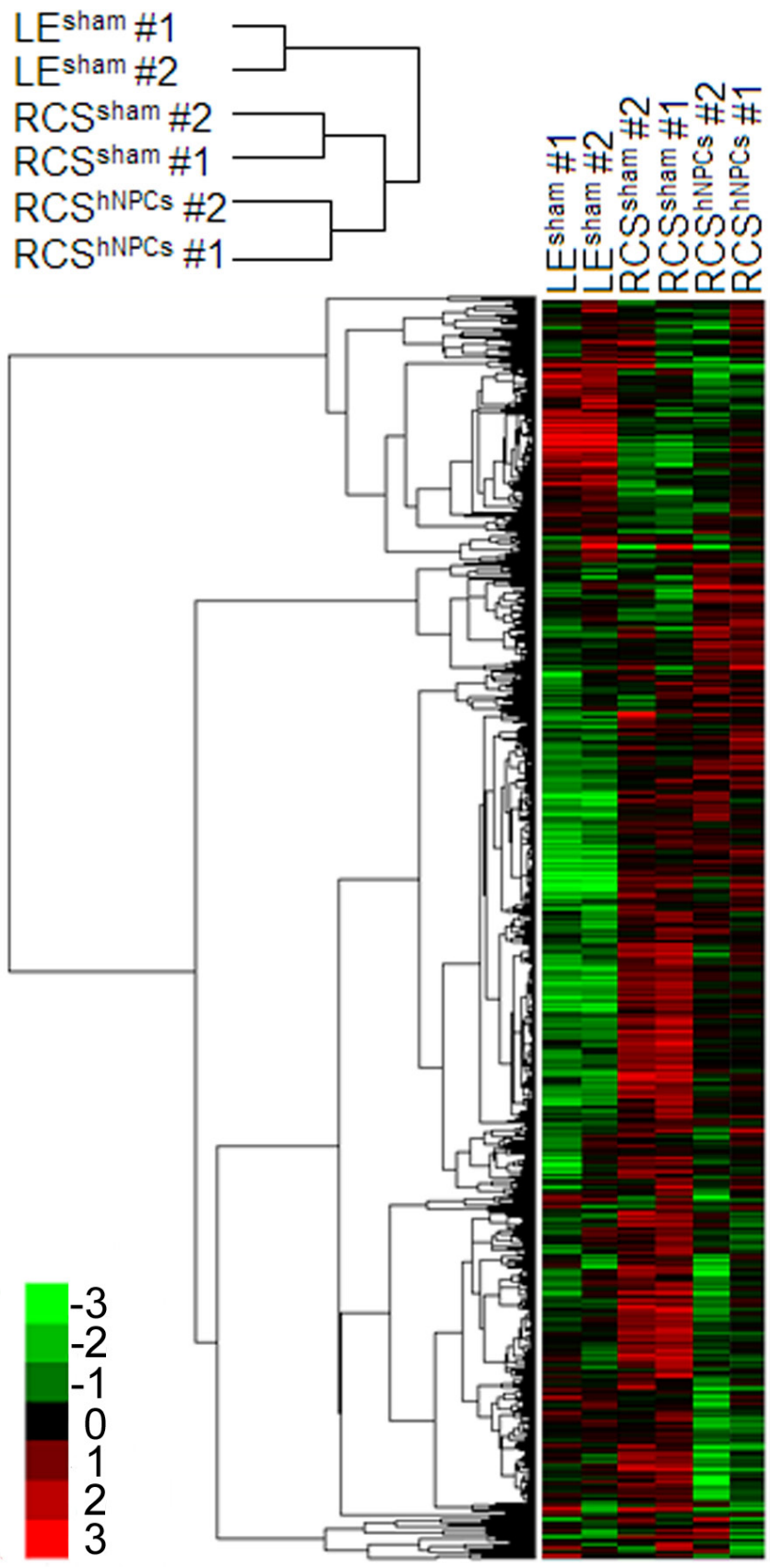

Figure 2. Hierarchical cluster analysis displays gene expression changes in LE^{sham}, RCS^{sham}, and RCS^{hNPCs} rats. Gene expression profiles of wild-type Long Evans (LE^{sham}, n = 2) rats were compared to retinal degenerate Royal College of Surgeons (RCS^{sham}, n = 2) rats and RCS rats with a subretinal injection of human forebrain derived neural progenitor cells (RCS^{hNPCs}, n = 2).

Table 1. Sequences for primers used in qRT-PCR.

Primer Name	Sequence	Primer Name	Sequence
ActBL	TGTCACCAACTGGGACGATA	Pax4R	GTGTCTTCAGGCAGAGAGGT
ActBR	GGGGTGTTGAAGGTCTCAAA	PdcL	ACCGCTTTTCCTCAGACGTA
Amigo2L	TGCCATGTTCCAGGAGCTAA	PdcR	GTTGGTCTGCCCTAGGTCAT
Amigo2R	AGATCAGCCAGCTTGAACCT	RhoL	GCAGTGTTCATGTGGGATTG
Cdc42ep5L	CAGTGTTAGGCGTCATGGAC	RhoR	CTGCCTTCTGAGTGGTAGCC
Cdc42ep5R	CAAAAGTGGAGTGCAGGGAG	Rp1L	CTTGTGGTGCCATGCTCATT
Cdh22L	GCTCTCTTGGTCTGTGTCCT	Rp1R	CCCTGAATGCCTACCTCCAT
Cdh22R	GTCATAAGCCTCGGTGTCCT	SeboxL	CTCTTCCAGACACTCCCCAG
Glb1l2L	GCTTCCTTCCTTCCTGTCCT	SeboxR	TTAGCCCCTGACCAACTCTG
Glb1l2R	CAGAAAATGCCCGTCCACAA	Ubald1L	CCTCTGTCTGCACCCCTAAA
Htr1fL	ACAACCACCATCAACTCCCT	Ubald1R	CACCCAAGCCACTTTGAGTC
Htr1fR	GTCACAGAGTCCTTGTCCCA	Ypel1L	TGGGCTCTCAGATTTTCCGT
Pax4L	GCTCTTCCTAGTCCCCACAG	Ypel1R	CCTTCTTCCTGCCTTTCTGC

by increasing sucrose before embedding in optimum cutting temperature (OCT) compound (Sakura Finetek, Torrance, CA) and storage at −80 °C. Horizontal sections were cut on a Leica CM1850 cryostat microtome (Leica Biosystems, Nussloch, Germany) at 10 µm per section. Four sections (50 µm apart)/slide were collected in five series, and every fifth slide was used for cresyl violet staining and imaged with a Leica DM6000B transmitted light microscope (Leica Microsystems, Wetzlar, Germany). For the RNA extraction experiments, the rats were euthanized with CO_2 followed by bilateral pneumothorax, and the eyes were briefly cleansed with ethanol before they were removed. Neural retinas were

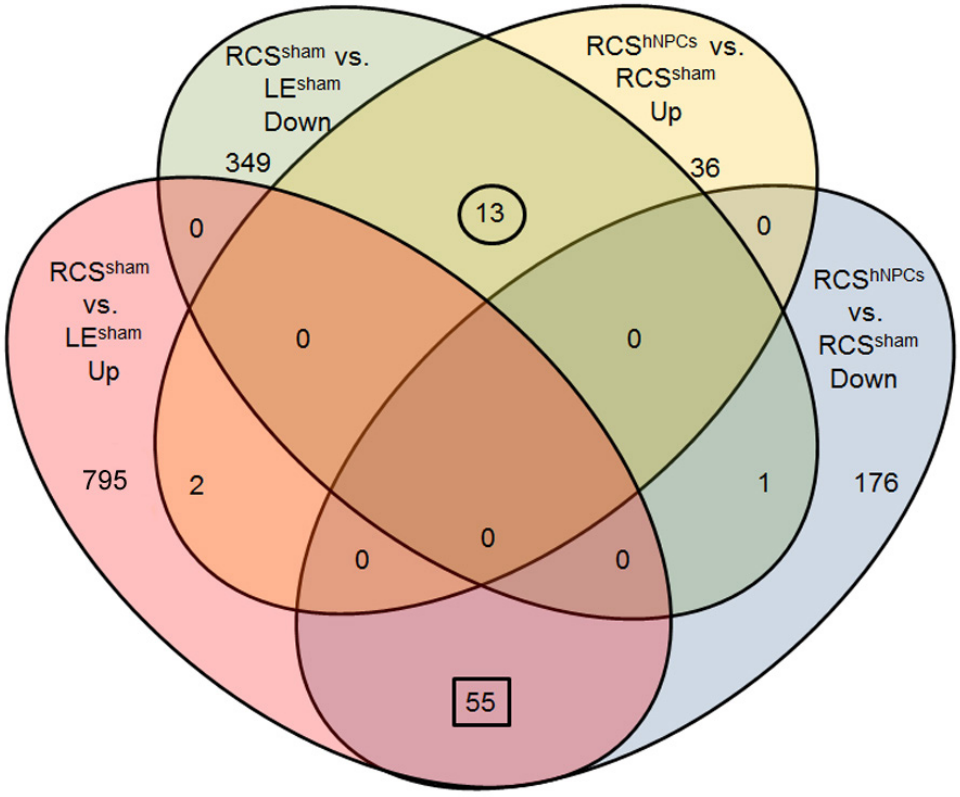

Figure 3. Comparison of differentially expressed gene sets reveals the presence of rescue genes. Up- and downregulated differentially expressed gene sets were determined for retinal degenerate Royal College of Surgeons (RCS^{sham}) rats versus wild-type Long Evans (LE^{sham}) rats and Royal College of Surgeons rats with a subretinal injection of human forebrain derived neural progenitor cells (RCS^{hNPCs}) rats versus RCS^{sham} rats and compared for overlapping genes. Genes with inverse relationships between the gene sets, termed rescued genes, were identified (circle and square).

Table 2. Numbers of expressed genes in LE^{sham}, RCS^{sham}, and RCS^{hNPCs}.

Sample	Total number of genes	Number of DE genes compared with RCSsham	Number of genes with higher expression in RCSsham	Number of genes with lower expression in RCSsham
LEsham	18,254	1215	852	363
RCSsham	18,662	-	-	-
RCshNPcs	18,627	283	232	51

Total number of genes is from mean of samples. Number of differentially expressed (DE) genes identified from each comparison of RCS^{sham} versus LE^{sham} and RCS^{hNPCs} versus RCS^{sham}. Significance was accepted at FDR q<0.05.

removed from the eye cup and oriented so that only the hemisphere containing the injected cells was isolated, flash frozen with liquid nitrogen, and stored at −80 °C until RNA extraction.

RNA isolation: Total RNA was extracted from individual halved neural retinas using the Purelink RNA Mini Kit (Life Technologies) according to the manufacturer's instructions. RNA quality was assessed using a NanoDrop ND-1000 spectrophotometer (NanoDrop Technologies, Wilmington, DE) and the Agilent 2100 system (Agilent Technologies, Santa Clara, CA).

RNA-sequencing (RNA-seq): Total RNA (1 µg) was poly-A selected using Dynabeads® Oligo(dT)25 (Life Technologies). cDNA libraries were constructed with barcoded primers using Ion Total RNA-Seq Kit v2 (Life Technologies), and were multiplexed and amplified onto ion sphere particles (ISPs) using Ion PI™ Template OT2 200 Kit v3 (Life Technologies). Libraries were sequenced to an average depth of 10 million reads/sample using the Ion PI™ Sequencing 200 Kit v3 (Life Technologies) by the Genomics Core at Cedars-Sinai Medical Center.

Bioinformatic analyses: Raw reads were filtered and trimmed with the FASTX toolkit and then were aligned to the rat reference genome rn5. Fragment per kilobase of gene per million reads sequenced (FPKM) values were calculated for 26,407 genes with Cufflinks 2.0.8 software [29]. Genes with sample FPKMs equaling 0 were excluded from further analyses. Sequence data were deposited in GEO per MIAME standards (accession number: GSE70600) [30,31]. All FPKM values were increased with an addition of 1, $\log_2$ transformed, and hierarchical cluster analysis of gene expression was performed with Cluster and TreeView software [32]. Differentially expressed genes were determined using a two-tailed t test, and were then corrected with calculation of the q value with the Benjamini-Hochberg method. Genes with significant expression differences with a false-discovery rate below 5% (q<0.05) were used for further analyses. Differential gene profiles (RCS^{sham} versus LE^{sham} and RCS^{hNPCs} versus RCS^{sham}) were compared for matching genes. Rescue genes were defined as those common between upregulated RCS^{sham} versus LE^{sham} and downregulated RCS^{hNPCs} versus RCS^{sham} or downregulated RCS^{sham} versus LE^{sham} and upregulated RCS^{hNPCs} versus RCS^{sham}. To determine the degree to which the genes were rescued, the fold changes between the two sets were then added to yield a fold change difference and were sorted based on values closest to 0. Functional annotation clustering analysis of the differentially expressed gene lists (RCS^{sham} versus LE^{sham} up- and downregulated and RCS^{hNPCs} versus RCS^{sham} up- and downregulated) were performed by submission to the Database for Annotation, Visualization and Integrated Discovery (DAVID v6.7) [33,34], and Gene Ontology (GO) term significance was accepted at Benjamini-Hochberg <0.001. Pie charts were generated using Microsoft Excel using the activation scores. Biologic processes and cellular components were determined by submission of the aforementioned differentially expressed gene lists to the Gene Ontology enRIchment anaLysis and visuaLizAtion tool (GOrilla) [35,36] for GO term analysis, and subsequently submitted to REViGO online software for visualization [37]. For canonical pathway analysis, differentially expressed genes from each gene list were submitted to the Ingenuity Pathway Analysis (IPA) Spring 2015 Release software (QIAGEN, Redwood City, CA), and significance was accepted with a –log Fisher's exact test p≥1.3 and a z score of ≥2 or ≤–2.

qRT-PCR: The top five characterized rescue genes from the gene list in the square in Figure 3 and the top six rescue genes from the genes in the circle in Figure 3 were further analyzed with quantitative real-time polymerase chain reaction (qRT-PCR) for expression validation. Total RNA was extracted from isolated halved neural retina samples of three biologic replicates each of LE^{sham}, RCS^{sham}, and RCS^{hNPCs} as described above. RCS^{sham} and RCS^{hNPCs} retinas were taken from the same animals, corresponding to the left and right eyes, respectively. cDNA synthesis was performed using the High-Capacity cDNA Reverse Transcription Kit (Life Technologies) according to the manufacturer's instructions.

The qRT-PCR analyses were performed using 50 ng cDNA on 96-well plates (Applied Biosystems, Paisley, UK), and run in technical duplicates on a 7500 Real-Time PCR System (Applied Biosystems). The ΔΔCt method was used to calculate fold changes, using ActB as a housekeeping standard and the LE^{sham} sample as the calibrator. Primers were designed with Primer3 online software [38,39] and selected to amplify fragments with 150–250 bp and with a Tm of approximately 60 °C (Table 1). Primers were designed for the following gene targets: *Actb* (NM_031144), *Amigo2* (NM_182816), *Cdc42ep5* (NM_001108469), *Cdh22* (NM_019161), *Htr1f* (NM_021857), *Pax4* (NM_031799), *Pdc* (NM_012872), *Rp1* (NM_001195676), *Sebox* (NM_023951), *Ubald1* (NM_001007668), and *Ypel1* (XM_002727914). To ensure accurate qRT-PCR expression patterns, primers were also designed and used for rhodopsin (NM_033441), which is expressed in photoreceptors.

RESULTS

Preservation of photoreceptors and visual function following hNPC treatment: At P21, wild-type LE rats received sham surgery (LE^{sham}), while retinal degenerate RCS rats received sham surgery (RCS^{sham}) in one eye and a subretinal injection of hNPCs (RCS^{hNPCs}) into the fellow eye. To ensure functional benefit, the OKR test measured the relative visual acuity of the LE^{sham}, RCS^{sham}, and RCS^{hNPCs} eyes at age P60. The OKR measurements for the LE^{sham} eyes were 0.6350 ± 0.0020 c/d, compared to a significant decrease to 0.3245 ± 0.0047 c/d in the RCS^{sham} eyes ($p<0.001$) and a subsequent significant increase to 0.4503 ± 0.0064 c/d in RCS^{hNPCs} eyes ($p<0.001$; Figure 1A). Following OKR analysis, eyes were enucleated and fixed for histological analysis. To confirm that hNPCs aided in photoreceptor survival, retinal cross sections were stained with cresyl violet dye (Figure 1B–D). The LE^{sham} eyes had approximately ten layers of photoreceptor cells located in the outer nuclear layer (ONL; Figure 1B), whereas the number of photoreceptor cells decreased to only three layers in the RCS^{sham} eyes (Figure 1C). In the RCS^{hNPCs} eyes, transplanted hNPCs survived in the subretinal space and were able to preserve approximately five to six cell layers of photoreceptors (Figure 1D). Similar to previous studies [10-12], the hNPCs were able to preserve visual function and aid in photoreceptor survival.

Analysis of global gene expression: To examine the overall gene expression in the host retinal tissue, retinal RNA was isolated (n = 2 for each of LE^{sham}, RCS^{sham}, and RCS^{hNPCs}), and RNA-seq was performed. Expression levels of 26,407 RefSeq protein-coding genes using the FPKM values was determined. A complete list of genes is registered at GEO (accession GSE70600). Only genes with expression of FPKM >0 were included for analysis. The total number of expressed genes for each sample was similar, with an average number of 18,254 (69%) in LE^{sham}, 18,662 (71%) in RCS^{sham}, and 18,627 (71%) in RCS^{hNPCs} (Table 2). To compare the similarity of the global gene expression profiles of the different samples, average linkage hierarchical cluster analysis was performed (Figure 2). The LE^{sham} samples clearly separated from the RCS samples, suggesting that there is a distinct difference in gene expression between wild-type and degenerating retinas. These data are in agreement with other transcriptomic studies of animal models for retinal degeneration [24,25]. Additionally, the RCS^{hNPCs} samples segregated from the RCS^{sham} samples indicating that distinguishable gene expression changes follow injection of hNPCs.

Differential gene expression in retinal degenerative RCS rats: To investigate gene expression changes with retinal degeneration, computational analysis of the differential gene expression between RCS^{sham} and LE^{sham} was performed. Genes were considered to be differentially expressed with an FDR <5% (q <0.05). A total of 1,215 differentially expressed genes were identified in the RCS^{sham} versus LE^{sham} comparison (Table 1; Appendix 1). Of these genes, 852 (70%) genes had increased expression in the RCS^{sham} samples (Figure 3, red ellipse), and 82 genes (10%) were uncharacterized. The top five genes with the greatest fold changes included *Mir671*, *Lcn2*, *Cd74*, *Gfap*, and *Cebpd*. *Lcn2*, *Cd74*, *Gfap*, and *Cebpd* have all been shown to be increased with retinal degeneration [15,19,25,40-45], confirming retinal degeneration is detectable at the molecular level. Additionally, *Mir671*, *Lcn2*, *Cd74*, and *Cebpd* play roles in the immune response to macrophages and/or microglia [45-48], suggesting that there is an increase in macrophage/microglia activity with retinal degeneration.

Of the 1,215 differentially expressed genes in the RCS^{sham} versus LE^{sham} comparison, 363 (30%) genes had decreased expression in the RCS^{sham} samples (Figure 3 green ellipse), and 29 (8%) were uncharacterized. The top five genes with the greatest fold change were *Optc*, *Gnat1*, *Hk2*, *Lig4*, and *Nrl*. *Gnat1*, *Hk2*, and *Nrl* are expressed in photoreceptors [46-53], and *Rho* (rhodopsin) was also greatly decreased with a fold change of −6.4, indicating that there is a significant decrease in photoreceptor-specific genes in the RCS^{sham} samples. This corroborates with the loss of photoreceptors in the retinal histology (Figure 1C). *Optc*, *Gnat1*, *Hk2*, *Lig4*, and *Nrl* have either been implicated in human retinal degenerative diseases [54-58] or are used in animal models for vision disorders [24,50,52], further establishing that retinal degeneration is discernible on the gene expression level.

Differential gene expression due to hNPC-induced retinal preservation in RCS rats: Computational analysis of the differential gene expression between RCS^{hNPCs} and RCS^{sham} was performed. A total of 283 differentially expressed genes were identified in the RCS^{hNPCs} versus RCS^{sham} comparison (Table 1; Appendix 2). A total of 51 (18%) genes had increased expression (Figure 3, yellow ellipse), and 21 (41%) of these genes are uncharacterized, suggesting that many of the genes expressed following hNPC treatment are currently unidentifiable. The top genes with greatest fold changes were *Mir671*, *ENSRNOG00000049107*, *Pde4d*, *Anxa9*, and *Mir770*. As previously described, *Mir671* is expressed in response to macrophage/microglia activity but also plays a role in regulating extracellular matrix production [59]. Downregulation of *Pde4d* and *Anxa9* expression is observed in retinal degeneration [24,60,61], and the increase in expression in this data set indicates that there is less retinal degeneration in RCS^{hNPCs}. *Mir770* is ubiquitously expressed in the mouse eye at P60 [62], and this may be further elucidated by looking at the target genes of this microRNA.

Of the 283 differentially expressed genes between RCS^{hNPCs} and RCS^{sham}, 232 (82%) genes had decreased expression in the RCS^{hNPCs} samples (Figure 3, blue ellipse). Similar to the upregulated RCS^{hNPCs} versus RCS^{sham} gene set, a high percentage of genes (79; 34%) are uncharacterized. The top five most downregulated genes include *Cryaa*, *Tomm6*, *ENSRNOG00000050736*, *Crybb3*, and *Cryba1*. The expression of crystallin genes, such as *Cryaa*, *Crybb3*, and *Cryba1*, is altered following retinal trauma and may play a protective role [63-68]. Decreased crystallin expression in RCS^{hNPCs} may be due to increased photoreceptor survival and less need for endogenous retinal neuroprotection. *Tomm6* encodes a protein that is part of the TOM complex of the mitochondrial membrane [69], and altered expression of TOM complex proteins has been detected in patients with diabetic retinopathies [70]. Collectively, the downregulation of these genes suggests that there is less retinal injury following treatment with hNPCs.

Functional, biologic, and cellular component analyses of differential gene expression sets: To identify functional processes that are affected, gene profiles were submitted to DAVID [33,34]. Of the 852 upregulated differentially expressed genes in the RCS^{sham} versus LE^{sham} comparison, ten functional processes were identified (Figure 4A). These genes were heavily associated with immune and inflammatory responses, suggesting that there is an increase in the immune response in the RCS^{sham} samples. The remaining functional processes participate in motility, suggesting there is an increase in the transportation of proteins across the cell and in cellular movement. Functional analysis of the 363 downregulated genes from the RCS^{sham} versus LE^{sham} comparison identified four significantly enriched pathways (Figure 4B). The downregulation of these processes (visual perception, phototransduction, photoreceptor cell development and differentiation, and detection of visible light) further confirm that retinal degeneration is detectable on a molecular basis in the RCS^{sham} samples. To determine the affected functional processes with treatment of hNPCs, the differentially expressed gene sets from the RCS^{hNPCs} versus RCS^{sham} comparisons were submitted to DAVID. The 51 upregulated genes yielded two processes (protein biosynthesis and cytosol; Figure 4C), and no processes were enriched using the downregulated genes. The lack of processes may be due to the small number of genes submitted to DAVID or the high percentage of uncharacterized genes in the RCS^{hNPCs} versus RCS^{sham} comparison.

To determine gene relation to biologic processes, GO terms from the differential gene expression profiles were submitted to REViGO. Similar to the functional analysis

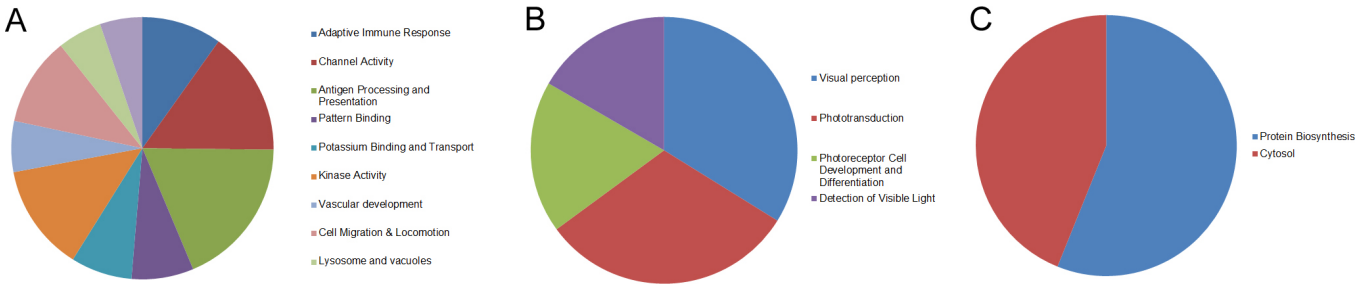

Figure 4. Analysis of affected functional processes in differential gene expression lists. Gene lists were submitted for DAVID analysis, and affected functional processes from the retinal degenerate Royal College of Surgeons (RCS^{sham}) versus wild-type Long Evans (LE^{sham}) upregulated (**A**) and downregulated (**B**) gene sets, and the Royal College of Surgeons rats with a subretinal injection of human forebrain derived neural progenitor cells (RCS^{hNPCs}) versus RCS^{sham} upregulated (**C**) gene list were identified. No significant functional processes were found for the RCS^{hNPCs} versus RCS^{sham} downregulated gene set. Significance was accepted at a Benjamini-Hochberg p value of less than 0.01.

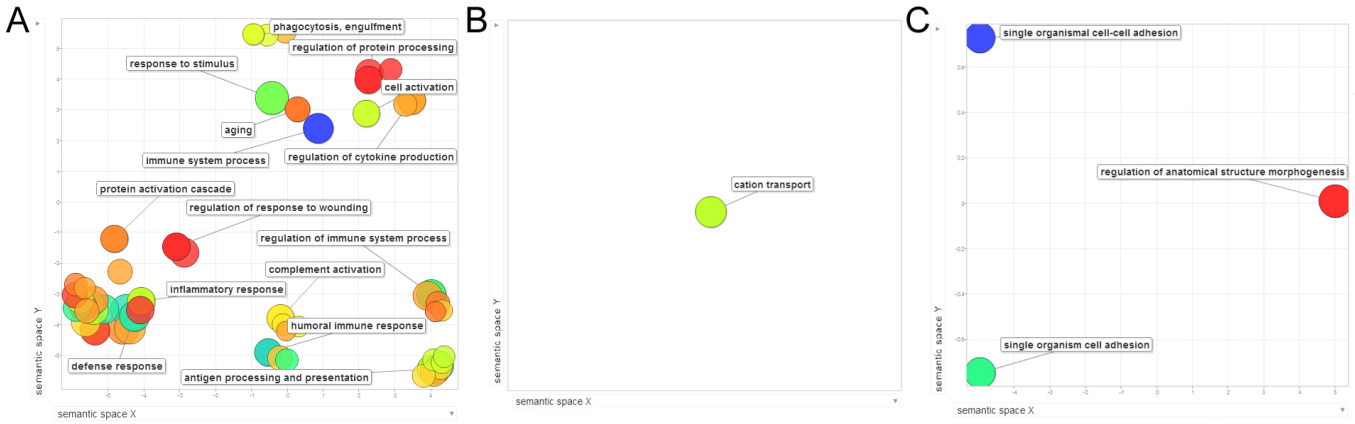

Figure 5. Scatterplot of biologic processes generated from differentially expressed genes. Gene Ontology (GO) terms from the differential gene expression lists were submitted to the REViGO web server. GO terms are represented by circles and are plotted according to similarity to other GO terms, and size is proportional to frequency of the GO term. Circle color defines the log10 p value (red is larger, blue is smaller). **A**: The retinal degenerate Royal College of Surgeons (RCS^{sham}) versus wild-type Long Evans (LE^{sham}) upregulated gene list produced several affected biologic processes. **B**: Only one process was identified in the downregulated gene list. **C**: The Royal College of Surgeons rats with a subretinal injection of human forebrain derived neural progenitor cells (RCS^{hNPCs}) versus RCS^{sham} upregulated gene list identified three affected processes, and no processes from the downregulated gene set. Significance was accepted at a Benjamini-Hochberg p value of less than 0.01.

by DAVID, the RCS^{sham} versus LE^{sham} upregulated biologic processes mainly included immune system regulation (Figure 5A). This analysis further demonstrates that the immune response is heightened in RCS^{sham}. The downregulated differentially expressed gene list from RCS^{sham} versus LE^{sham} procured only one biologic process (Figure 5B). Cation transport is important for the directed movement of molecules between or within cells, and the downregulation of this process may be linked to the decreases of photoreceptor cells and in phototransduction. To identify biologic processes that are affected following treatment with hNPCs, GO terms from the RCS^{hNPCs} versus RCS^{sham} differentially expressed gene lists were submitted to REViGO. Three biologic processes were determined from the upregulated gene list (Figure 5C). These processes participate in cell adhesion and regulation of morphogenesis, which could be due to the increase in rescued photoreceptors. The genes from the downregulated gene set could not be classified into any significantly enriched biologic processes.

The differential gene lists were also analyzed for cellular component ontology, which describes where the gene product is located in the cell. Submission of GO terms from the RCS^{sham} versus LE^{sham} upregulated gene list identified five cellular components (Figure 6A). These components suggest that the abundance of immune cells is increased in the RCS^{sham} samples. The downregulated gene list from RCS^{sham} versus LE^{sham} yielded one cellular component (cilium; Figure 6B). Photoreceptor outer segments are characterized as specialized sensory cilia [71], and RCS^{sham} have a defect in phagocytosing outer segments [26]. Additionally, inherited retinal degenerative diseases can be linked to cilia mutations [72], further demonstrating that retinal degeneration can be detected at the molecular level in RCS^{sham}. No significant cellular components were established in either of the RCS^{hNPCs} versus RCS^{sham} comparisons.

Rescue gene expression in RCS^{hNPCs}: RCS^{hNPCs} were shown to have increased visual function and photoreceptor cell survival (Figure 1). To analyze genes that may be aiding in these processes, computational analysis of the differential gene sets between the comparisons was conducted, and rescue genes were identified (Figure 3, circle). Fifty-five genes common to the upregulated RCS^{sham} versus LE^{sham} and downregulated RCS^{hNPCs} versus RCS^{sham} gene lists were identified (Figure 3, square, Appendix 3). To determine genes with RCS^{hNPCs} expression similar to that of LE^{sham}, the fold change difference (FCD) was calculated. FCD was defined as ((RCS^{sham} versus LE^{sham} fold change) + (RCS^{hNPCs} versus RCS^{sham} fold change). The top characterized genes with an FCD closest to 0 are *Ubald1* (FCD 0.02) *Sebox* (FCD −0.02), *Cdh22* (FCD −0.02), *Amigo2* (FCD −0.03), and *Cdc42ep5* (FCD 0.04). To date, there are no publications on the expression of *Ubald1* or *Sebox* in the retina. *Amigo2* is expressed in the rat retina [73], and *Cdh22* is expressed in the developing mouse brain [74], but little is known about their biologic relevance. *Cdc42* is important for tissue organization during retinal development, and loss of *Cdc42* results in retinal degeneration [75,76].

Cdc42ep5 encodes an effector protein that binds to Cdc42 to negatively regulate its function [77,78]. The decrease in *Cdc42ep5* expression in RCS^{hNPCs} may allow for more Cdc42 expression and subsequent retinal preservation.

To further evaluate rescue genes, the downregulated RCS^{sham} versus LE^{sham} and upregulated RCS^{hNPCs} versus RCS^{sham} were compared. A total of 13 genes were identified (Figure 3, circle), and the top rescue genes with an FCD closest to 0 are *Htr1f* (FCD −0.14), *Ypel1* (FCD −0.17), *Pdc* (FCD −0.36), *Glbl12* (FCD 0.47), and *Pax4* (FCD 0.50; Appendix 4). *Htr1f* was found to have higher expression in the temporal retina than in the macular retina of human patients [79]. *Ypel1* may play a role in regulation of cell morphology [80] and/or in cell division [81], but no expression analysis in the retina has been performed. *Pdc* (phosducin) is highly expressed in photoreceptors [82,83], suggesting that there is a significant increase in photoreceptor gene expression in RCS^{hNPCs}. *Glbl12* is ubiquitously expressed in the eye, including the retina, and may play a role in retinal cell homeostasis [84]. *Pax4* is expressed in photoreceptors [85] and can stimulate expression of the rod-derived cone viability factor for photoreceptor survival [86,87]. Collectively, the upregulation of these rescue genes indicate that there is an increase in photoreceptor gene expression following treatment with hNPCs.

Validation of differential gene expression: qRT-PCR analysis was performed on the genes with an FCD closest to 0 from each of the lists of rescued genes. Of the rescued genes that were upregulated in the RCS^{sham} versus LE^{sham} and downregulated in the RCS^{hNPCs} versus RCS^{sham} sets (Appendix 3), one of the five genes (*Cdc42ep5*) followed similar gene expression patterns as seen in the RNA-seq expression (Figure 7A). As described previously, the downregulation of *Cdc42ep5* expression in RCS^{hNPCs} may be due to photoreceptor preservation. Of the rescued genes that were downregulated in the RCS^{sham} versus LE^{sham} and upregulated in the RCS^{hNPCs} versus RCS^{sham} sets (Appendix 4), all six genes (*Htr1f*, *Ypel1*, *Pdc*, *Glbl12*, *Pax4*, and *Rp1*) followed similar expression patterns as those detected in the RNA-seq analysis (Figure 7B). To confirm the histological analysis, the photoreceptor gene rhodopsin (*Rho*) was also included in qRT-PCR analysis.

Pathway analysis of rescued genes following hNPC transplantation: To determine which pathways may be rescued following transplantation of hNPCs into the RCS rat, gene lists were uploaded into the Ingenuity Pathway Analysis (IPA) software. All of the genes that were significantly upregulated

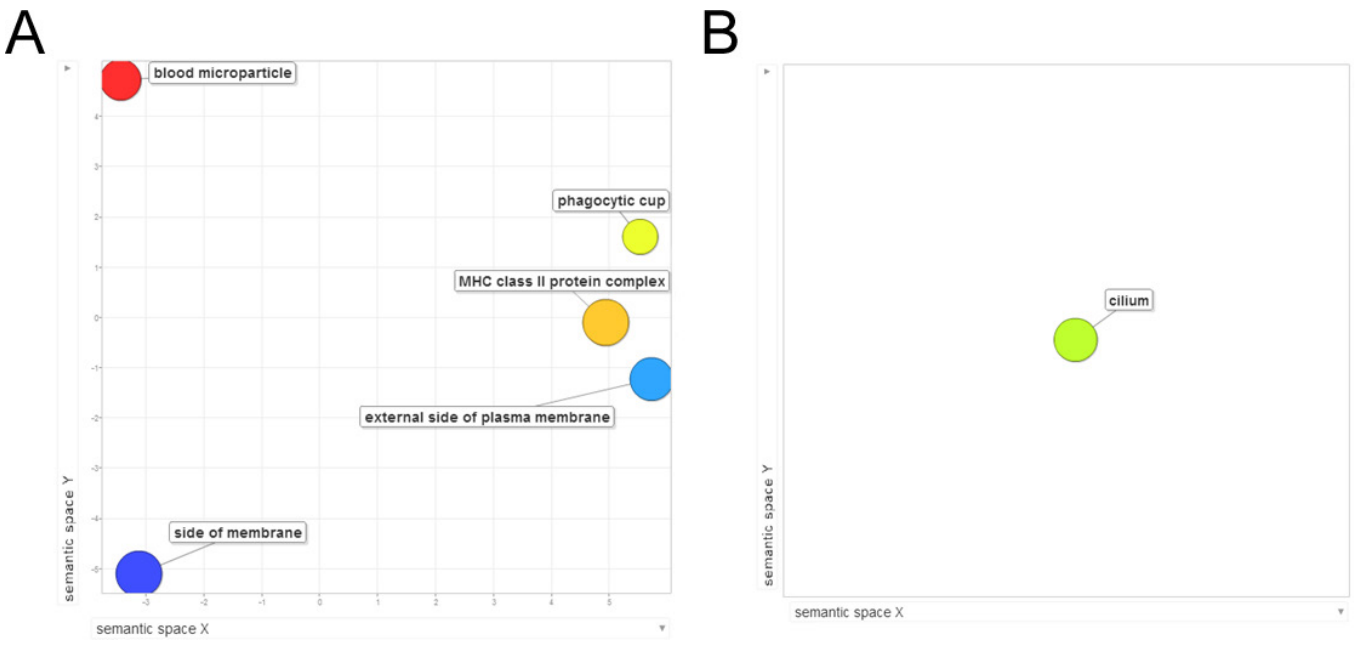

Figure 6. Scatterplot of gene product cellular components generated from differentially expressed genes. Gene Ontology (GO) terms from the differential gene expression lists were submitted to the REViGO web server. GO terms are represented by circles and are plotted according to similarity to other GO terms, and size is proportional to frequency of the GO term. Circle color defines the log10 p value (red is larger, blue is smaller). **A**: The retinal degenerate Royal College of Surgeons (RCS^{sham}) versus wild-type Long Evans (LE^{sham}) upregulated gene list produced five affected cellular components. **B**: Only one process was identified in the downregulated gene list. No significant cellular components were identified in either of the Royal College of Surgeons rats with a subretinal injection of human forebrain derived neural progenitor cells (RCS^{hNPCs}) versus RCS^{sham} gene lists. Significance was accepted at a Benjamini-Hochberg p value of less than 0.01.

in the RCS^{sham} versus LE^{sham} and downregulated in the RCS^{h-NPCs} versus RCS^{sham} gene profiles were compared, and three pathways were found to coincide (Table 3). Integrin signaling is involved in promotion of inflammation [88] and the uptake of apoptotic cells by macrophages and microglia [89]. The second affected pathway, phospholipase C signaling, is important for efficient phagocytosis [90], which is one function of macrophages and microglia. The third pathway, Rho Family GTPase signaling, promotes phagocytic engulfment [91]. The importance of the three pathways coincides with the functional, biologic, and cellular components analyses that indicated that there is an increased immune response in RCS^{sham} (Figure 4, Figure 5). The three affected pathways all play roles in the phagocytic response, suggesting that the host RCS^{sham} retina is infiltrated with macrophages and microglia. Fewer macrophages and microglia may be due to less degenerative materials or less stress on photoreceptors targeted for phagocytosis, since photoreceptors are preserved with hNPC treatment. No pathways were identified in the downregulated RCS^{sham} versus LE^{sham} and upregulated RCS^{h-NPCs} versus RCS^{sham} comparison.

Decrease in abundance of macrophages and microglia following hNPC treatment: Comparison of the pathways affected by the gene sets suggest phagocytosis signaling as the common biologic process by which all three pathways participate. To determine whether the presence of macrophages and microglia contributes to the overall gene expression changes, immunofluorescent staining was performed (Figure 8). A greater amount of positive staining for Iba1, a marker of macrophages and microglia, was detected in the RCS^{sham} retina (Figure 8B) compared to the LE^{sham} retina (Figure 8A). Treatment with hNPCs decreased the amount of positive staining in areas with rescued photoreceptors (Figure 8C), similar to the expression patterns detected in the LE^{sham} retina. Similar to RCS^{sham} expression, areas away from the grafted region of the treated retina had an increase in macrophages and microglia (Figure 8D), suggesting that the decrease in the abundance of macrophages and microglia is directly due to the presence of hNPCs.

DISCUSSION

Effective therapies for RDDs, such as retinitis pigmentosa and age-related macular degeneration, remain a challenge from a clinical perspective, and many questions still surround the use of stem cell–based therapies. This study enhances the knowledge of gene expression changes that occur following injection of human neural progenitor cells into a clinically relevant rodent model for retinal degeneration. By comparing

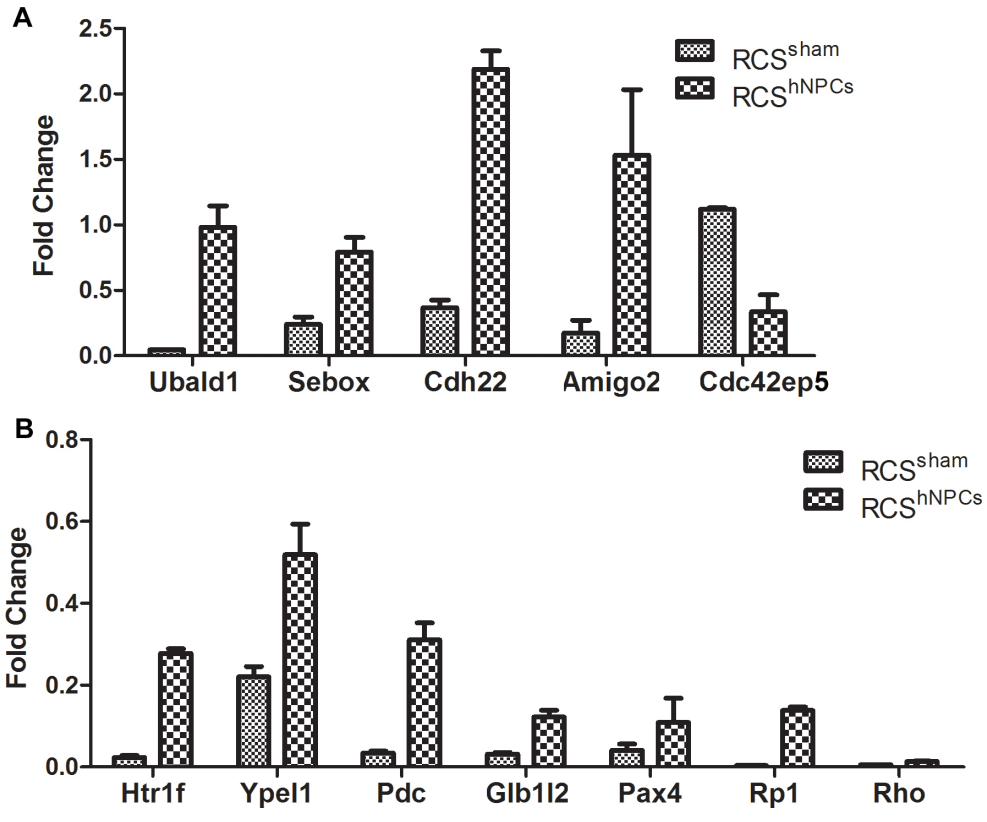

Figure 7. Validation of rescue gene expression using qRT-PCR analysis. Primers were designed for rescue genes with a fold change difference (FCD) closest to 0. **A**: The top five retinal degenerate Royal College of Surgeons (RCS^{sham}) versus wild-type Long Evans (LE^{sham}) downregulated and Royal College of Surgeons rats with a subretinal injection of human forebrain derived neural progenitor cells (RCS^{hNPCs}) versus RCS^{sham} upregulated rescue genes. The top six RCS^{sham} versus LE^{sham} upregulated and RCS^{hNPCs} versus RCS^{sham} downregulated rescue genes were examined. **B**: The photoreceptor-specific gene rhodopsin (*Rho*) was also probed.

Table 3. Ingenuity pathway analysis (IPA) of differential gene expression lists.

Gene List	Canonical Pathway	-log(*p*-value)	z-score	Gene IDs
RCS^{sham} vs. LE^{sham} Upregulated	Integrin Signaling	3.79	4.123	ACTA1, ACTB, ARPC1B, ITGA6, ITGA9, ITGAL, ITGAM, ITGB2, PARVA, PIK3CG, RAC2, RAP2B, RHOB, RHOC, RHOJ, RRAS, SRC, TSPAN4
RCS^{hNPCs} vs. RCS^{sham} Downregulated	Integrin Signaling	1.54	-2.000	ARPC1A, PARVA, RHOB, RRAS
RCS^{sham} vs. LE^{sham} Upregulated	Phospholipase C Signaling	2.14	3.606	BLNK, FCER1G, FCGR2A, FCGR2B, GNB3, GNG5SRC, LYN, PLCE1, PLD4, RHOB, RHOC, RHOJ, RRAS, SYK, TGM
RCS^{hNPCs} vs. RCS^{sham} Downregulated	Phospholipase C Signaling	1.31	-2.000	GNG5, PLA2G1B, RHOB, RRAS
RCS^{sham} vs. LE^{sham} Upregulated	Signaling by Rho Family GTPases	2.6	3.873	ACTA1, ACTB, ARPC1B, CDC42EP5, CDH11, EZR, FOX, GFAP, GNB3, GNG5, JUN, MSNRHOC, PIK3CG, RHOB, RHOJ, SEPT10
RCS^{hNPCs} vs. RCS^{sham} Downregulated	Signaling by Rho Family GTPases	1.94	-2.000	ARPC1A, CDC42EP5, GFAP, GNG5, RHOB

Upregulated RCS^{sham} versus LE^{sham} and downregulated RCS^{hNPCs} versus RCS^{sham} gene lists were compared. Significance was determined at –log p value ≥1.31 and z-score ≥2 or ≤ −2. Gene IDs shown are those that were found to be differentially expressed in the data set as determined by IPA software (QIAGEN, Redwood City).

the degenerating retina to the hNPC-treated retina, greater knowledge of the responses that occur due to hNPCs will aid in understanding the molecular mechanisms of treatment. Challenges arise from determining exact signaling mechanisms in heterogeneous tissue. Because a multitude of cell types constitute the retina, it is difficult to attribute exact gene expression differences to specific cells. However, this whole neural retinal approach is useful for determining global changes to the retina, and certain signaling mechanisms may be extrapolated from this data set and further studied on a cell-specific basis.

Previous studies from our laboratory have determined that hNPCs are able to preserve vision and aid in photoreceptor survival in RCS rats [10-12]. The use of hNPCs in humans could yield great promise for treating retinal degenerative diseases, but the mechanisms of action of stem cell–based therapies are largely undiscovered. Previous studies on induced pluripotent stem cell-derived neural progenitor cells (iNPCs) and fetal-derived central nervous stem cells (HuCNS-SC) have shown that neural stem cells are able to phagocytose debris in the subretinal space, suggesting one mechanism of the benefit of neural stem cells [15,16]. Other potential mechanisms have been postulated, such as neurotrophic factor release and immunomodulation, but there has been little evidence of the exact modes of action of stem cell therapies. This is the first study to examine the changes in the host retina following stem cell therapy, and this knowledge could be used to enhance future applications for treatment.

The RNA-seq data suggest several different gene expression changes among LE^{sham}, RCS^{sham}, and RCS^{hNPCs}. These data sets are based on contributions of gene expression changes from the whole retina. While not taking into account minute changes in specific cells, further studies could examine the differences in cell subtypes to further pinpoint gene expression changes. One concern is that the area of the retina used for analysis also contains hNPCs, which could contribute to the overall gene expression changes. Studies in our laboratory have shown that hNPCs constitute approximately 1% of the RCS retinal cells at P60, as determined with flow cytometry (unpublished lab data). Transcript levels from the hNPCs themselves were therefore not considered to greatly contribute to the gene expression differences seen in the host retinal tissue RNA-seq.

Although compelling increases in photoreceptor cell survival occurs in RCS^{hNPCs}, interestingly, Rho was not found in the genes that were significantly increased from the RCS^{hNPCs} versus RCS^{sham} comparison. The fold change was 1.5 from RCS^{hNPCs} to RCS^{sham}; thus, although there are more photoreceptors with treatment with hNPCs, Rho is not detected in the gene expression changes. The low levels of rhodopsin in

the RNA-seq and qRT-PCR analyses of RCS^{hNPCs} could be due to the sample area of the neural retina. The area closest to the injection site, approximately half of the neural retina, was taken to maximize the hNPC-induced photoreceptor survival, but the sample also contains portions of the retina that are not affected by hNPCs thus potentially decreasing the overall rhodopsin gene expression levels. However, other photoreceptor-specific genes were found to be significantly upregulated with hNPC treatment. They include *Rs1* (FC = 2.1, q = 0.007) for retinal organization [92], *Pdc* (FC = 2.3, q = 0.03) expressed in photoreceptors [82,83], *Rp1* (FC = 2.3, 1 value 0.02) for stacking of outer segment discs [93], and *Rpgrip1* (FC = 2.3, q = 0.02), which is expressed in photoreceptor cells [94].

Gene expression changes from the RNA-seq were validated using qRT-PCR. Although not all of the genes were validated, *Cdc42ep5* expression was confirmed and was also found to be important in the bioinformatic pathway analysis. Potentially the small sample size for the qRT-PCR was not adequate for detecting the subtle fold-change differences between the different groups, and using a larger number of biologic samples could improve validation efforts. There was also variability between the biologic samples, and it could not be ascertained how great the photoreceptor preservation was in each sample, which could skew the expression patterns. In addition, the genes that could not be validated with qRT-PCR were mainly from the upregulated RCS^{sham} versus LE^{sham} and downregulated RCS^{hNPCs} versus RCS^{sham} rescue gene list. Smaller subtle fold-change differences (range from −0.03 to 0.04) from this rescued gene list, compared to the downregulated RCS^{sham} versus LE^{sham} and upregulated RCS^{hNPCs} versus RCS^{sham} rescued genes (range from −0.64 to 0.5), may be harder to be accurately detected. Additionally, the fold changes themselves in the former rescue genes list were smaller (up to 2.82 and −2.69) compared to the ones that were validated in the latter rescue gene list (up to −3.48 and 3.39).

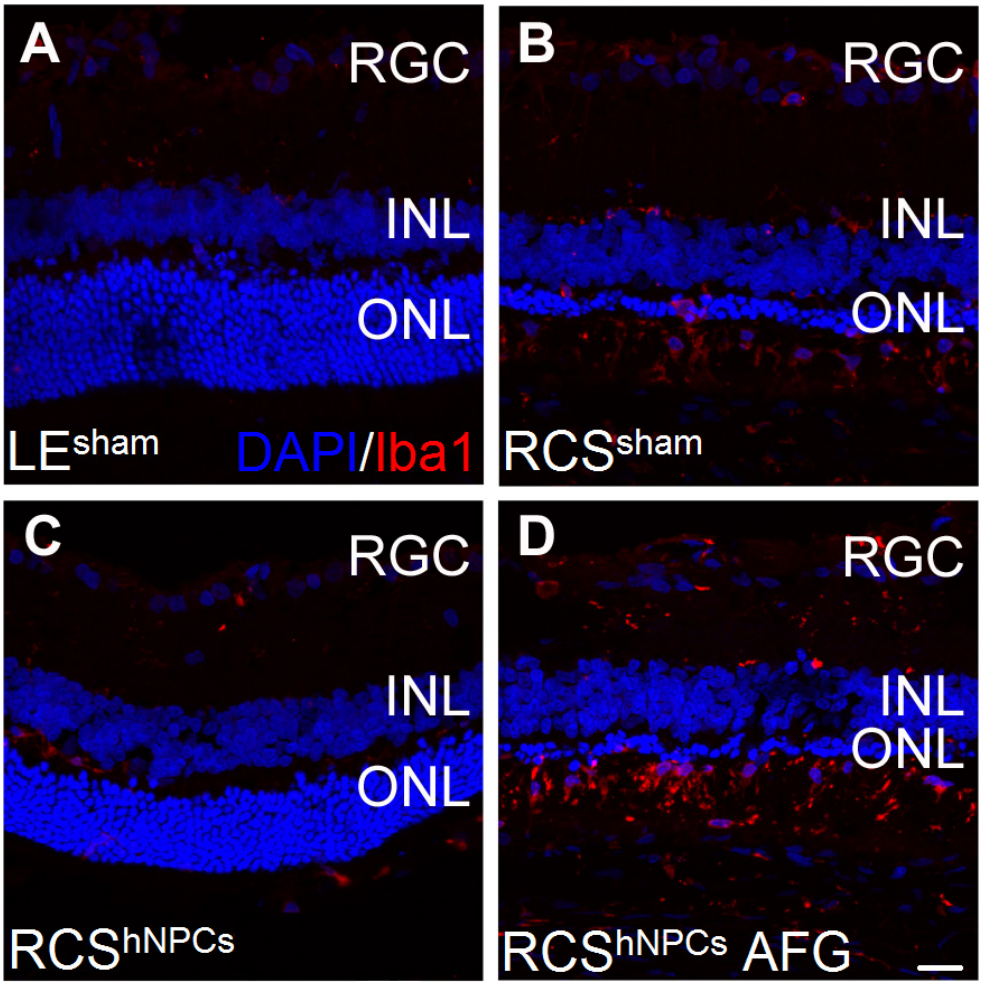

Figure 8. The presence of macrophages and microglia decreases after hNPC treatment. **A**: Wild-type Long Evans (LE^{sham}) have few macrophages and microglia, as detected with the Iba1 antibody. **B**: Retinal degenerate Royal College of Surgeons (RCS^{sham}) have Iba1+ cells throughout the retina. **C**: Similar to LE^{sham}, Royal College of Surgeons rats with a subretinal injection of human forebrain derived neural progenitor cells (RCS^{hNPCs}) have few Iba1+ cells. **D**: However, areas further from the injection site away from the graft (AFG) with less photoreceptor survival contain numerous macrophage and microglial cells. RGC = retinal ganglion cell layer, INL = inner nuclear layer, ONL = outer nuclear layer. Scale bar = 20 µm.

Pathway analysis was used to identify affected pathways following the subretinal transplantation of hNPCs into RCS rats. Although no pathways were found to be significantly affected in the downregulated RCS^{sham} versus LE^{sham} and upregulated RCS^{hNPCs} versus RCS^{sham} comparisons, pathways that were found to be affected were the phototransduction (-log Benjamini-Hochberg p = 2.49E01), visual cycle (4.34E00), retinoate biosynthesis (1.96E00), and retinal biosynthesis (1.96E00) pathways. The only pathway that had a significant z score was the cardiac β-adrenergic signaling pathway (-log Benjamini-Hochberg p = 1.95E00, z score = −2). This pathway includes the genes *Pde8a*, *Gnb1*, *Pde6g*, *Pde6a*, *Gnb5*, and *Pde6b*. These genes were also found in the phototransduction pathway, suggesting that certain aspects of the phototransduction pathway are affected but did not reach significance by such stringent analysis.

Three pathways were found to be significantly affected in the upregulated RCS^{sham} versus LE^{sham} and downregulated RCS^{hNPCs} versus RCS^{sham} comparisons. The first pathway, integrin signaling, is essential for synchronizing phagocytosis of photoreceptor outer segments by the retinal pigment epithelial cells [95,96]. The RCS rats have a mutation in the *MerTK* gene that cause a truncation of the Mertk protein and improper phagocytosis of the photoreceptor outer segments [26]. *MerTK* is activated by pathways controlled by signaling via the αvβ5 integrin receptor [96]. Improper phagocytosis of photoreceptor outer segments can lead to retinal degeneration [97,98], and loss of αvβ5 integrin allows phagocytosis to occur but at an improper rate [99] and leads to vision loss [98,100]. The upregulation of integrin signaling factors in the RCS^{sham} versus LE^{sham} comparison could be integrin signaling compensation by RPE cells due to the lack of functional Mertk protein; however, the RNA-seq samples were composed of the neural retina with few RPE cells, suggesting alternate cells in the retina utilize integrin signaling for phagocytosis. Integrin receptors are also expressed on macrophages and microglia and are involved in the uptake of apoptotic targets [89] and the promotion of inflammation [88]. Inhibition of integrin receptors blocked microglial function and reduced phagocytosis of apoptotic neurons [89]. hNPCs potentially block the action of macrophages and microglia either directly by signaling to the phagocytic cells or indirectly by increasing photoreceptor survival, thus decreasing the need for phagocytosis of apoptotic cells.

The second affected pathway is phospholipase C (PLC) signaling. The PLC signaling cascade affects several cellular processes, including metabolism, secretion, phagocytosis, proliferation, and neurotransmission [101]. Activation of phagocytic receptors, such as integrins, activate PLC signaling resulting in elevated Ca^{2+} concentrations in the cytosol, which is required for maturation of phagosomes and efficient phagocytosis [90]. In cooperation with Rho family GTPase signaling, the third affected pathway, macrophages are activated and play a role in actin turnover and rearrangement [102,103] to promote phagocytic engulfment [91]. Microglial infiltration and activation have been detected in RCS rats over the course of retinal degeneration [104], which was also identified in RCS^{sham} (Figure 8B). Microglial activity is detrimental to the survival of photoreceptors, and suppression of microglial activity lessens vision loss [105-107]. Microglia also aid in the execution of stressed, living photoreceptors and other neurons [108,109], further contributing to neurodegeneration. A decrease in the presence of macrophages and microglia was observed in in RCS^{hNPCs} in areas with photoreceptor survival (Figure 8C), and macrophages and microglia were again detected in areas of the same eye that had less photoreceptor survival (Figure 8D). In RCS^{hNPCs} areas away from the injection site, there was no sham surgery effect, and it is similar to what is seen in eyes that received no surgery or treatment. The ONL thickness is approximately two to three cell layers in the RCS^{sham} (Figure 8B), whereas the RCS^{hNPCs} area away from the injection site (Figure 8D) has approximately one to two cell layers. The increased Iba1 staining in the RCS^{hNPCs} area away from the injection site could be due to more photoreceptor degeneration, therefore causing the presence or increased activity of macrophages and microglia. These data suggest that one neuroprotective effect of hNPCs on retinal degeneration is due to modulating the response of macrophages and microglia in areas of photoreceptor survival.

In conclusion, this is the first report of RNA-seq transcriptome data that shows gene expression following treatment of a clinically relevant stem cell source, hNPCs, in a rodent model for retinal degeneration. The differential gene expression data of RCS^{sham} versus LE^{sham} retinas expands the knowledge of the progression of retinal degeneration, while the analysis of RCS^{hNPCs} versus RCS^{sham} gives insight into potential genes and pathways that may be targeted in future therapeutic studies. Furthermore, these results are the first to demonstrate that hNPCs induce immunomodulation in the retina, either by directly signaling to immune cells or indirectly by aiding in photoreceptor survival thereby inactivating immune cells. Gene expression data sets, such as the present study, will elucidate biologic and molecular relevance of therapies in retinal degenerative diseases, with the hope of generating more efficacious therapeutics.

APPENDIX 1.

Genes with differential expression between the RCS^{sham} and LE^{sham} samples. To access the data, click or select the words "Appendix 1."

APPENDIX 2.

Genes with differential expression between the RCS^{hNPCs} and RCS^{sham} samples. To access the data, click or select the words "Appendix 2."

APPENDIX 3.

Rescue genes upregulated in RCS^{sham} versus LE^{sham} and downregulated in RCS^{hNPCs} versus RCS^{sham} comparisons. Numbers given are fold changes between the two listed samples. Fold change difference (FCD) was determined as ((RCS^{sham} versus LE^{sham} fold change) + (RCS^{hNPCs} versus RCS^{sham} fold change). To access the data, click or select the words "Appendix 3."

APPENDIX 4.

Rescue genes downregulated in RCS^{sham} versus LE^{sham} and upregulated in RCS^{hNPCs} versus RCS^{sham} comparisons. Numbers given are fold changes between the two listed samples. Fold change difference (FCD) was determined as ((RCS^{sham} versus LE^{sham} fold change) + (RCS^{hNPCs} versus RCS^{sham} fold change). To access the data, click or select the words "Appendix 4."

ACKNOWLEDGMENTS

The authors thank Lindsay Spurka and Dr. Vincent Funari from the Cedars-Sinai Genomics Core for support with the RNA-seq. The authors also acknowledge the laboratories of Dr. Clive Svendsen and Dr. Barry Stripp for assistance, and Lin Shen for technical support. This work was supported by funding from the NEI (R01EY020488), California Institute for Regenerative Medicine (LSP1–08235), and Cedars-Sinai Medical Center Board of Governors Regenerative Medicine Institute. A portion of this study was submitted for presentation at the 2016 Association for Research in Vision and Ophthalmology annual meeting in Seattle, WA.

BIBLIOGRAPHY

1. Ben M'Barek K, Regent F, Monville C. Use of human pluripotent stem cells to study and treat retinopathies. World J Stem Cells 2015; 7:596-604. [PMID: 25914766].
2. Mansergh FC, Carrigan M, Hokamp K, Farrar GJ. Gene expression changes during retinal development and rod specification. Mol Vis 2015; 21:61-87. [PMID: 25678762].
3. Hobbs RP, Bernstein PS. Nutrient supplementation for age-related macular degeneration, cataract, and dry eye. J Ophthalmic Vis Res 2014; 9:487-93. [PMID: 25709776].
4. Zampatti S, Ricci F, Cusumano A, Marsella LT, Novelli G, Giardina E. Review of nutrient actions on age-related macular degeneration. Nutr Res 2014; 34:95-105. [PMID: 24461310].
5. Dewan A, Liu M, Hartman S. HTRA1 promoter polymorphism in wet age-related macular degeneration. Science 2006; 314:989-92. [PMID: 17053108].
6. Fritsche LG, Loenhardt T, Janssen A, Fisher SA, Rivera A, Keilhauer CN, Weber BHF. Age-related macular degeneration is associated with an unstable ARMS2 (LOC387715) mRNA. Nat Genet 2008; 40:892-6. [PMID: 18511946].
7. Yu Y, Bhangale TR, Fagerness J, Ripke S, Thorleifsson G, Tan PL, Souied EH, Richardson AJ, Merriam JE, Buitendijk GH, Reynolds R, Raychaudhuri S, Chin KA, Sobrin L, Evangelou E, Lee PH, Lee AY, Leveziel N, Zack DJ, Campochiaro B, Campochiaro P, Smith RT, Barile GR. Guymer Rh, Hogg R, Chakravarthy U, Robman LD, Gustafsson O, Sigurdsson H, Ortmann W, Behrens TW, Stefansson K, Uitterlinden AG, van Duijn CM, Vingerling JR, Klaver CC, Allikmets R, Brantley MA Jr, Baird PN, Katsanis N, Thorsteinsdottir U, Ioannidis JP, Daly MJ, Graham RR, Seddon JM. Common variants near FRK/COL10A1 and VEGFA are associated with advanced age-related macular degeneration. Hum Mol Genet 2011; 20:3699-709. [PMID: 21665990].
8. McHarg S, Clark SJ, Day AJ, Bishop PN. Age-related macular degeneration and the role of the complement system. Mol Immunol 2015; 67:43-50. [PMID: 25804937].
9. Garcia JM, Mendonca L, Brant R, Abud M, Regatieri C, Diniz B. Stem cell therapy for retinal diseases. World J Stem Cells 2015; 7:160-4. [PMID: 25621115].
10. Wang S, Girman S, Lu B, Bischoff N, Holmes T, Shearer R, Wright LS, Svendsen CN, Gamm DM, Lund RD. Long-term vision rescue by human neural progenitors in a rat model of photoreceptor degeneration. Invest Ophthalmol Sci 2008; 49:3201-6. [PMID: 18579765].
11. McGill TJ, Cottam B, Lu B, Wang S, Girman S, Tian C, Huhn SL, Lund RD, Capela A. Transplantation of human central nervous system stem cells – neuroprotection in retinal degeneration. Eur J Neurosci 2012; 35:468-77. [PMID: 22277045].
12. Lu B, Lin Y, Tsai Y, Girman S, Adamus G, Jones MK, Shelley B, Svendsen CN, Wang S. A subsequent human neural progenitor transplant into the degenerate retina does not compromise initial graft survival or therapeutic efficacy. Transl Vis Sci Technol 2015; 4:7-[PMID: 25694843].
13. Francis PJ, Wang S, Zhang Y, Brown A, Huang T, McFarland TJ, Jeffrey BG, Lu B, Wright L, Appukuttan B, Wilson DJ, Stout JT, Neuringer M, Gamm DM, Lund RD. Subretinal transplantation in forebrain progenitor cells in nonhuman primates: Survival and intact retinal function. Invest Ophthalmol Sci 2009; 50:3425-31. [PMID: 19234356].
14. Gamm DM, Wang S, Lu B, Girman S, Holmes T, Bischoff T, Bischoff N, Shearer RL, Sauve Y, Capowski E, Svendsen CN,

Lund RD. Protection of visual functions by human neural progenitors in a rat model of retinal disease. PLoS One 2007; 28:e338-[PMID: 17396165].

15. Tsai Y, Lu B, Bakondi B, Girman S, Sahabian A, Sareen D, Svendsen CN, Wang S. Human iPSC-derived neural progenitors preserve vision in an AMD-like model. Stem Cells 2015; •••:[PMID: 25869002].

16. Cuenca N, Fernandez-Sanchez L, McGill TJ, Lu B, Wang S, Lund R, Huhn S, Capela A. Phagocytosis of photoreceptor outer segments by transplanted human neural stem cells as a neuroprotective mechanism in retinal degeneration. Invest Ophthalmol Vis Sci 2013; 54:6745-56. [PMID: 24045996].

17. Lee T. Host tissue response in stem cell therapy. World J Stem Cells 2010; 2:61-6. [PMID: 21031156].

18. Pluchino S, Cossetti C. How stem cells speak with host immune cells in inflammatory brain diseases. Glia 2013; 61:1379-401. [PMID: 23633288].

19. Wang S, Lu B, Girman S, Duan J, McFarland T, Zhang QS, Grompe M, Adamus G, Appukuttan B, Lund R. Non-invasive stem cell therapy in a rat model for retinal degeneration and vascular pathology. PLoS One 2010; 5:e9200-[PMID: 20169166].

20. Scalinci SZ, Scorolli L, Corradetti G, Domanico D, Vingolo EM, Meduri A, Bifani M, Siravo D. Potential role of intravitreal human placental stem cell implants in inhibiting progression of diabetic retinopathy in type 2 diabetes: neuroprotective growth factors in the vitreous. Clin Ophthalmol 2011; 5:691-6. [PMID: 21629576].

21. Malliaras K, Ibrahim A, Tseliou E, Liu W, Sun B, Middleton RC, Seinfeld J, Wang L, Sharifi BG, Marban E. Stimulation of endogenous cardioblasts by exogenous cell therapy after myocardial infarction. EMBO Mol Med 2014; 6:760-77. [PMID: 24797668].

22. Radeke MJ, Peterson KE, Johnson LV, Anderson DH. Disease susceptibility of the human macula: Differential gene transcription in the retinal pigmented epithelium/choroid. Exp Eye Res 2007; 85:366-80. [PMID: 17662275].

23. Newman AM, Gallo NB, Hancox LS, Miller NJ, Radeke CM, Maloney MA, Cooper JB, Hageman GS, Anderson DH, Johnson LV, Radeke MJ. Systems-level analysis of age-related macular degeneration reveals global biomarkers and phenotype-specific functional networks. Genome Med 2012; 4:16-[PMID: 22364233].

24. Kozhevnikova OS, Korbolina EE, Ershov NI, Kolosova NG. Rat retinal transcriptome Effects of aging and AMD-like retinopathy. Cell Cycle 2013; 12:1745-61. [PMID: 23656783].

25. Uren PJ, Lee JT, Doroudchi MM, Smith AD, Horsager A. A profile of transcriptomic changes in the rd10 mouse model of retinitis pigmentosa. Mol Vis 2014; 20:1612-28. [PMID: 25489233].

26. D'Cruz PM, Yasumra D, Weir J, Matthes MT, Abderrahim H, LaVail MM, Vollrath D. Mutation of the receptor tyrosine kinase gene Mertk in the retinal dystrophic RCS rat. Hum Mol Genet 2000; 9:645-51. [PMID: 10699188].

27. Vollrath D, Feng W, Duncan JL, Yasumra D, D'Cruz PM, Chappelow A, Matthes MT, Kay MA, LaVail MM. Correction of the retinal dystrophy phenotype of the RCS rat by viral gene transfer of Mertk. Proc Natl Acad Sci USA 2001; 98:12584-9. [PMID: 11592982].

28. Gal A, Li Y, Thompson DA, Weir J, Orth U, Jacobson SG, Apfelstedt-Sylla E, Vollrath D. Mutations in MERTK, the human orthologue of the RCS rat retinal dystrophy gene, cause retinitis pigmentosa. Nat Genet 2000; 26:270-1. [PMID: 11062461].

29. Trapnell C, Roberts A, Goff L, Pertea G, Kim D, Kelly DR, Pimentel H, Salzberg SL, Rinn JL, Pachter L. Differential gene and transcript expression analysis of RNA-seq experiments with TopHat and Cufflinks. Nat Protoc 2012; 7:562-78. [PMID: 22383036].

30. Brazma A, Hingamp P, Quackenbush J, Sherlock G, Spellman P, Stoeckert C, Aach JU, Ansorge W, Ball CA, Causton HC, Gaasterland T, Glenisson P, Holstege FC, Kim IF, Markowitz V, Matese JC, Parkinson H, Robinson A, Sarkans U, Schulze-Kremer S, Stewart J, Taylor R, Vilo J, Vingron M. Minimum information about a microarray experiment (MIAME – toward standards for microarray data). Nat Genet 2001; 29:365-71. [PMID: 11726920].

31. Brazma A. Minimum information about a microarray experiment (MIAME – successes, failures, challenges). ScientificWorldJournal 2009; 9:420-3. [PMID: 19484163].

32. Eisen MB, Spellman PT, Brown PO, Botstein D. Cluster analysis and display of genome-wide expression patterns. Proc Natl Acad Sci USA 1998; 95:14863-8. [PMID: 9843981].

33. Huang DW, Sherman BT, Lempicki RA. Bioinformatics enrichment tools: paths toward the comprehensive functional analysis of large gene lists. Nucleic Acids Res 2009; 37:1-13. [PMID: 19033363].

34. Huang DW, Sherman BT, Lempicki RA. Systematic and integrative analysis of large gene lists using DAVID Bioinformatics Resources. Nat Protoc 2009; 4:44-57. [PMID: 19131956].

35. Eden E, Lipson D, Yogev S, Yakhini Z. Discovering motifs in ranked lists of DNA sequences. PLOS Comput Biol 2007; 3:e39-[PMID: 17381235].

36. Eden E, Navon R, Steinfeld I, Lipson D, Yakhini Z. GOrilla: a tool for discovery and visualization of enriched GO terms in ranked gene lists. BMC Bioinformatics 2009; 10:48-[PMID: 19192299].

37. Supek F, Bosnjak M, Skunca N, Smuc T. REVIGO summarizes and visualizes long lists of gene ontology terms. PLoS One 2011; 6:e21800-[PMID: 21789182].

38. Koressaar T, Remm M. Enhancements and modifications of primer design program Primer3. Bioinformatics 2007; 23:1289-91. [PMID: 17379693].

39. Untergrasser A, Cutcutache I, Koressaar T, Ye J, Faircloth BC, Remm M, Rozen SG. Primer3 – new capabilities and interfaces. Nucleic Acids Res 2012; 50:e115-[PMID: 22730293].

40. Lewis GP, Fisher SK. Up-regulation of glial fibrillary acidic protein in response to retinal injury: its potential role in glial remodeling and a comparison to vimentin expression. Int Rev Cytol 2003; 230:263-90. [PMID: 14692684].

41. Chang ML, Wu CH, Jiang-Shieh YF, Shieh JY, Wen CY. Reactive changes of retinal astrocytes and Muller glial cells in kainite-induced neuroexcitotoxicity. J Anat 2007; 210:54-65. [PMID: 17229283].

42. Rattner A, Toulabi L, Williams J, Yu H, Nathans J. The genomic response of the retinal pigment epithelium to light damage and retinal detachment. Neurobiol Dis 2008; 23:9880-9. [PMID: 18815272].

43. Samardzija M, Wariwoda H, Imsand C, Huber P, Heynen SR, Gubler A, Grimm C. Activation of survival pathways in the degenerating retina of rd10 mice. Exp Eye Res 2012; 99:17-26. [PMID: 22546314].

44. Wang J, Lin J, Schlotterer A, Wu L, Fleming T, Busch S, Dietrich N, Hammes HP. CD74 indicates microglial activation in experimental diabetic retinopathy and exogenous methylglyoxal mimics the response in normoglycemic retina. Acta Biabetol 2014; 51:813-21. [PMID: 24974304].

45. Kolibabka M, Weinold C, Busch S, Margerie D, Hammes HP, Molema G. Lipocalin-2 in degenerative retinopathy. Diabetologie und Sstoffwechesel 2015; 10:76-.

46. Steele MR, Inman DM, Calkins DJ. Microarray analysis of retinal gene expression in the DBA/2J model of glaucoma. Invest Ophthalmol Vis Sci 2006; 47:977-85. [PMID: 16505032].

47. Lien GH, Liu JF, Chien MH, Hsu WT, Chang TH, Ku CC. J ATQ, Hsieh TL, Lee LM, Ho JH. The ability to suppress macrophage-mediated inflammation in orbital fat stem cells is controlled by miR-671–5p. Stem Cell Res Ther 2014; 5:97-[PMID: 25124290].

48. Valapala M, Edwards M, Hose S, Grebe R, Butto IA, Cano M, Berger T, Mak TW, Wawrousek E, Handa JT, Lutty GA, Zigler JS, Sinha D. Increased lipocalin-2 in the retinal pigment epithelium of Cryba1 cKO mice is associated with a chronic inflammatory response. Aging Cell 2014; 13:1091-4. [PMID: 25257511].

49. Khanna H, deNicola R, Hicks D, Swaroop A. Regulation of NRL expression by retinoic acid and trophic factors. Invest Ophthalmol Sci 2003; 44:3543-.

50. Maeda T, Cideciyan AV, Maeda A, Golczak M, Aleman TS, Jacobson SG, Palczewski K. Loss of cone photoreceptors caused by chromophore depletion is partially prevented by the artificial chromophore pro-drug, 9-cis-retinyl acetate. Hum Mol Genet 2009; 18:2277-87. [PMID: 19339306].

51. Reidel B, Thompson JW, Farsiu S, Moseley MA, Skiba NP, Arshavsky VY. Proteomic profiling of a layered tissue reveals unique glycolytic specializations of photoreceptor cells. Mol Cell Proteomics 2011; 10:M110-[PMID: 21173383].

52. Barber AC, Hippert C, Duran Y, West EL, Bainbridge JWB, Warre-Cornish K, Luhmann UFO, Lakowski J, Sowden JC, Ali RR, Pearson RA. Repair of the degenerate retina by photoreceptor transplantation. Proc Natl Acad Sci USA 2013; 110:354-9. [PMID: 23248312].

53. Farkas MH, Grant GR, White JA, Sousa ME, Consugar MB, Pierce EA. Transcriptome analyses of the human retina identify unprecedented transcript diversity and 3.5 Mb of novel transcribed sequence via significant alternative splicing and novel genes. BMC Genomics 2013; 14:486-[PMID: 23865674].

54. Bessant DAR, Payne AM, Mitton KP, Wang QL, Swain PK, Plant C, Bird AC, Zack DJ, Swaroop A, Bhattacharya SS. A mutation in NRL is associated with autosomal dominant retinitis pigmentosa. Nat Genet 1999; 21:355-6. [PMID: 10192380].

55. Friedman JS, Ducharme R, Raymond V, Walter MA. Isolation of a novel iris-specific and leucine-rich repeat protein (oculoglycan)using differential selection. Invest Ophthalmol Vis Sci 2000; 41:2059-66. [PMID: 10892843].

56. Hobby P, Wyatt MK, Gan W, Bernstein S, Tomarev S, Slingsby C, Wistow G. Cloning, modeling, and chromosomal localization for a small leucine-rich repeat proteoglycan (SLRP) family member expressed in human eye. Mol Vis 2000; 6:72-8. [PMID: 10837509].

57. DeAngelis MM, Grimsby JL, Sandberg MA, Berson EL, Dryja TP. Novel mutations in the NRL gene and associated clinical findings in patients with dominant retinitis pigmentosa. Arch Ophthalmol 2002; 120:369-75. [PMID: 11879142].

58. Sullivan LS, Koboldt DC, Bowne SJ, Lang S, Blanton SH, Cadena E, Avery CD, Lewis RA, Webb-Jones K, Wheaton K, Wheaton DH, Birch DG, Coussa R, Ren H, Lopez I, Chakarova C, Koenekoop RK, Garcia CA, Fulton RS, Wilson RK, Weinstock GM, Daiger SP. A dominant mutation in hexokinase (HK1) causes retinitis pigmentosa. Invest Ophthalmol Vis Sci 2014; 55:7147-58. [PMID: 25190649].

59. Rutnam ZJ, Yang BB. The non-coding 3′UTR of CD44 induces metastasis by regulating extracellular matrix functions. J Cell Sci 2012; 125:2075-85. [PMID: 22637644].

60. Bowes C, Li T, Danciger M, Baxter LC, Applebury ML, Farber DB. Retinal degeneration in the rd mouse is caused by defect in the beta subunit of rod cGMP-phosphodiesterase. Nature 1990; 347:677-80. [PMID: 1977087].

61. Kirin M, Chandra A, Charteris DG, Hayward C, Campbell S, Celap I, Bencic G, Vatavuk Z, Kirac I, Richards AJ, Tenesa A, Snead MP, Fleck BW, Singh J, Harsum S, Maclaren RE, den Hollander AI, Dunlop MG, Hoyng CB, Wright AF, Campbell H, Vitart V, Mitry D. Genome-wide association study identifies genetic risk underlying primary rhegmatogenous retinal detachment. Hum Mol Genet 2013; 22:3174-85. [PMID: 23585552].

62. Karali M, Peluso I, Gennarino VA, Bilio M, Verde R, Lago G, Dolle P, Banfi S. miRNeye: a microRNA expression atlas of the mouse eye. BMC Genomics 2010; 11:715-[PMID: 21171988].

63. Cavusoglu N, Thierse D, Mohand-Said S, Chalmel F, Poch O, Van-Dorsselaer A, Sahel JA, Leveillard T. Differential proteomic analysis of the mouse retina: the induction of

crystalline proteins by retinal degeneration in the rd1 mouse. Mol Cell Proteomics 2003; 2:494-505. [PMID: 12832458].

64. Ahmed F, Brown KM, Stephan DA, Morrison JC, Johnson EC, Tomarev SI. Microarray analysis of changes in mRNA levels in the rat retina after experimental elevation of intraocular pressure. Invest Ophthalmol Vis Sci 2004; 45:1247-58. [PMID: 15037594].

65. Vasquez-Chona F, Song BK, Geisert EE Jr. Temporal changes in gene expression after injury in the rat retina. Invest Ophthalmol Vis Sci 2004; 45:2737-46. [PMID: 15277499].

66. Templeton JP, Nassr M, Vazquez-Chona F, Freeman-Anderson NE, Orr WE, Williams RW, Geisert EE. Differential response of C57BL/6J mouse and DBA/2J mouse to optic nerve crush. BMC Neurosci 2009; 10:90-[PMID: 19643015].

67. Kim BJ, Braun TA, Wordinger RJ, Clark AF. Progressive morphological changes and impaired retinal function associated with temporal regulation of gene expression after retinal ischemia/reperfusion injury in mice. Mol Neurodegener 2013; 8:21-[PMID: 23800383].

68. Templeton JP, Wang XD, Freeman NE, Ma Z, Lu A, Hejtmancik F, Geisert EE. A crystallin gene network in the mouse retina. Exp Eye Res 2013; 116:129-40. [PMID: 23978599].

69. Kato H, Mihara K. Identification of Tom5 and Tom6 in the preprotein translocase complex of human mitochondrial outer membrane. Biochem Biophys Res Commun 2008; 369:958-63. [PMID: 18331822].

70. Zhong Q, Kowluru RA. Diabetic retinopathy and damage to mitochondrial structure and transport machinery. Invest Ophthalmol Vis Sci 2011; 52:8739-46. [PMID: 22003103].

71. Liu Q, Zhang Q, Pierce E. Photoreceptor sensory cilia and inherited retinal degeneration. Adv Exp Med Biol 2010; 664:223-32. [PMID: 20238021].

72. Bandano JL, Mitsuma N, Beales PL, Katsanis N. The ciliopathies: an emerging class of human genetic disorders. Annu Rev Genomics Hum Genet 2006; 7:125-48. [PMID: 16722803].

73. Kuja-Panula J, Kiiltomaki M, Yamashiro T, Rouhiainen A, Rauvala H. AMIGO, a transmembrane protein implicated in axon tract development, defines a novel protein family with leucine-rich repeats. J Cell Biol 2003; 160:963-73. [PMID: 12629050].

74. Saarimaki-Vire J, Alitalo A, Partanen J. Analysis of Cdh22 expression and function in the developing mouse brain. Dev Dyn 2011; 240:1989-2001. [PMID: 21761482].

75. Heynen SR, Meneau I, Caprara C, Samardzija M, Imsand C, Levine EM, Grimm C. CDC42 is required for tissue lamination and cell survival in the mouse retina. PLoS One 2013; 8:e53806-[PMID: 23372671].

76. Choi SY, Baek JI, Zuo X, Kim SH, Dunaief JL, Lipschutz JH. Cdc42 and sec10 are required for normal retinal development in zebrafish. Invest Ophthalmol Vis Sci 2015; 56:3361-70. [PMID: 26024121].

77. Joberty G, Perlungher RR, Macara IG. The Borgs, a new family of Cdc42 and TC10 GTPase-interacting proteins. Mol Cell Biol 1999; 19:6585-97. [PMID: 10490598].

78. Joberty G, Perlungher RR, Sheffield PJ, Kinoshita M, Noda M, Haystead T, Macara IG. Borg proteins control septin organization and are negatively regulated by Cdc42. Nat Cell Biol 2001; 3:861-6. [PMID: 11584266].

79. Whitmore SS, Wagner AH, DeLuca AP, Drack AV, Stone EM, Tucker BA, Zeng S, Braun TA, Mullins RF, Scheetz TE. Transcriptomic analysis across nasal, temporal, and macular regions of human neural retina and RPE/choroid by RNA-Seq. Exp Eye Res 2014; 129:93-106. [PMID: 25446321].

80. Farlie P, Reid C, Wilcox S, Peeters J, Reed G, Newgreen D. Ypel1: a novel nuclear protein that induces an epithelial-like morphology in fibroblasts. Genes Cells 2001; 6:619-29. [PMID: 11473580].

81. Hosono K, Sasaki T, Minoshima S, Shimizu N. Identification and characterization of a novel gene family YPEL in a wide spectrum of eukaryotic species. Gene 2004; 340:31-43. [PMID: 15556292].

82. Herrmann R, Lobanova ES, Hammond T, Kessler C, Burns ME, Frishman LJ, Arshavsky VY. Phosducin regulates transmission at the photoreceptor-to-ON-bipolar cell synapse. J Neurosci 2010; 30:3239-53. [PMID: 20203183].

83. Belcastro M, Song H, Sinha S, Song C, Mathers PH, Sokolov M. Phosphorylation of phosducin accelerates rod recovery from transducing translocation. Invest Ophthalmol Vis Sci 2012; 53:3084-91. [PMID: 22491418].

84. Le Carre J, Schorderet DF, Cottet S. Altered expression of β-galactosidase-1-like protein 3 (Glb1l3) in the retinal pigment epithelium (RPE)-specific 65-kDa protein knockout mouse model of Leber's congenital amaurosis. Mol Vis 2011; 17:1287-97. [PMID: 21633714].

85. Rath MF, Bailey MJ, Kim JS, Coon SL, Klein DC, Moller M. Developmental and daily expression of the Pax4 and Pax6 homeobox genes in the rat retina: localization of Pax4 in photoreceptor cells. J Neurochem 2009; 108:285-94. [PMID: 19012751].

86. Reichman S, Kalathur RK, Lambard S, Ait-Ali N, Yang Y, Lardenois A, Ripp R, Poch O, Zack DJ, Sahel JA, Leveillard T. The homeobox gene CHX10/VSX2 regulates RdCVF promoter activity in the inner retina. Hum Mol Genet 2010; 19:250-61. [PMID: 19843539].

87. Ait-Ali N, Fridlich R, Millet-Puetl G, Clerin E, Delalande F, Jaillard C, Blond F, Perrocheau L, Reichman S, Byrne LC, Olivier-Bandini A, Bellalou J, Moyse E, Bouillaud F, Nicol X, Dalkara D, van Dorsselaer A, Sahel JA, Leveillard T. Rod-derived cone viability factor promotes cone survival by stimulating aerobic glycolysis. Cell 2015; 161:817-32. [PMID: 25957687].

88. Li L, Eter N, Heiduschka P. The microglia in healthy and diseased retina. Exp Eye Res 2015; 136:116-30. [PMID: 25952657].

89. Witting A, Muller P, Herrmann A, Kettenmann H, Nolte C. Phagocytic clearance of apoptotic neurons by microglia/brain macrophages in vitro: Involvement of lectin-, integrin-, and phosphatidylserine-mediated recognition. J Neurochem 2000; 75:1060-70. [PMID: 10936187].

90. Nunes P, Demaurex N. The role of calcium signaling in phagocytosis. J Leukoc Biol 2010; 88:57-68. [PMID: 20400677].

91. Mao Y, Finnemann SC. Regulation of phagocytosis by Rho GTPases. Small GTPases 2015; 6:89-99. [PMID: 25941749].

92. Byrne LC, Ozturk BE, Lee T, Fortuny C, Visel M, Dalkara D, Schaffer DV, Flannery JG. Retinoschisin gene therapy in photoreceptors, Muller glia or all retinal cells in the *RS1h*−/− mouse. Gene Ther 2014; 21:585-92. [PMID: 24694538].

93. Liu Q, Lyubarsky A, Skalet JH, Pugh EN Jr, Pierce EA. RP1 is required for the correct stacking of outer segment discs. Invest Ophthalmol Vis Sci 2003; 44:4171-83. [PMID: 14507858].

94. Pawlyk BS, Bulgakov OV, Liu X, Xu X, Adamian M, Sun X, Khani SC, Berson EL, Sandberg MA, Li T. Replacement gene therapy with a human RPGRIP1 sequence slows photoreceptor degeneration in a murine model of Leber congenital amaurosis. Hum Gene Ther 2010; 21:993-1004. [PMID: 20384479].

95. Finnemann SC, Bonilha VL, Marmorstein AD, Rodriquez-Boulan E. Phagocytosis of rod outer segments by retinal pigment epithelial cells requires α(v)β5 integrin for binding but not for internalization. Proc Natl Acad Sci USA 1997; 94:12932-7. [PMID: 9371778].

96. Nandrot EF, Anand M, Almeida D, Atabai K, Sheppard D, Finnemann SC. Essential role for mFG-E8 as ligand for αvβ5 integrin in diurnal retinal phagocytosis. Proc Natl Acad Sci USA 2007; 104:12005-10. [PMID: 17620600].

97. Gibbs D, Kitamoto J, Williams DS. Abnormal phagocytosis by retinal pigmented epithelium that lacks myosin VIIa, the Usher syndrome 1B protein. Proc Natl Acad Sci USA 2003; 100:6481-6. [PMID: 12743369].

98. Nandrot EF, Kim Y, Brodie SE, Huang X, Sheppard D, Finnemann SC. Loss of synchronized retinal phagocytosis and age-related blindness in mice lacking αvβ5 integrin. J Exp Med 2004; 200:1539-45. [PMID: 15596525].

99. Law AL, Parinot C, Chatagnon J, Gravez B, Sahel JA, Bhattacharya SS, Nandrog EF. Cleavage of Mer Tyrosine Kinase (MerTK) from the cell surface contributes to the regulation of retinal phagocytosis. J Biol Chem 2015; 290:4941-52. [PMID: 25538233].

100. Mallavarapu M, Finnemann SC. Neural retina and MerTK-independent apical polarity of αvβ5 integrin receptors in the retinal pigment epithelium. Adv Exp Med Biol 2010; 664:123-31. [PMID: 20238010].

101. Rajala RVS, Anderson RE. Focus on molecules: phosphatidylinositol-4,5-bisphosphate (PIP2). Exp Eye Res 2010; 91:324-5. [PMID: 20457154].

102. Tybulewicz VLJ, Henderson RB. Rho Family GTPases and their regulators in lymphocytes. Nat Rev Immunol 2009; 9:630-44. [PMID: 19696767].

103. Tuosto L, Capuano C, Muscolini M, Santoni A, Galandrini R. The multifaceted role of PIP2 in leukocyte biology. Cell Mol Life Sci 2015; 72:4461-74. [PMID: 26265181].

104. Liu Y, Yang X, Utheim TP, Guo C, Xiao M, Liu Y, Yin Z, Ma J. Correlation of cytokine levels and microglial cell infiltration during retinal degeneration in RCS rats. PLoS One 2013; 8:e82061-[PMID: 24349184].

105. Lewis GP, Chapin EA, Luna G, Linberg KA, Fisher SK. The fate of Muller's glia following experimental retinal detachment: nuclear migration, cell division, and subretinal glial scar formation. Mol Vis 2010; 16:1361-72. [PMID: 20664798].

106. Cebulla CM, Zelinka CP, Scott MA, Lubow M, Bingham A, Rasiah S, Mahmoud AM, Fischer AJ. A chick model of retinal detachment: Cone rich and novel. PLoS One 2012; 7:e4457-[PMID: 22970190].

107. Fischer AJ, Zelinka C, Milani-Nejad N. Reactive retinal microglia, neuronal survival, and the formation of retinal folds and detachments. Glia 2015; 63:313-27. [PMID: 25231952].

108. Brown GC, Neher JJ. Eaten alive! Cell death by primary phagocytosis: 'phagoptosis'. Trends Biochem Sci 2012; 37:325-32. [PMID: 22682109].

109. Zhao L, Zabel MK, Wang X, Ma W, Shah P, Fariss RN, Qian H, Parkhurst CN, Gan WB, Wong WT. Microglial phagocytosis of living photoreceptors contributes to inherited retinal degeneration. EMBO Mol Med 2015; 7:1179-97. [PMID: 26139610].

Articles are provided courtesy of Emory University and the Zhongshan Ophthalmic Center, Sun Yat-sen University, P.R. China. The print version of this article was created on 16 May 2016. This reflects all typographical corrections and errata to the article through that date. Details of any changes may be found in the online version of the article.